Sediment Delivery and Bedform Variability of the Lower Fraser River and Delta

by

Daniel P. Murphy

B.Sc., State University of New York at Oneonta, 2020

Thesis Submitted in Partial Fulfillment of the
Requirements for the Degree of
Master of Science

in the
Department of Geography
Faculty of Environment

SIMON FRASER UNIVERSITY
Spring 2023

Declaration of Committee

Name:	**Daniel P. Murphy**
Degree:	**Master of Science (Geography)**
Title:	**Sediment Delivery and Bedform Variability of the Lower Fraser River and Delta**
Committee:	**Chair:** **Geoff Mann** Professor, Geography
	Jeremy G. Venditti Supervisor Professor, Environmental Science
	Ryan W. Bradley Committee Member Adjunct Professor, Environmental Science
	Michael A. Church Examiner Professor Emeritus, Geography University of British Columbia

Abstract

Large lowland river and delta management requires an understanding of the sediment dynamics governing the system. The lower Fraser River sediment budget, an integral tool to sustainably manage the Fraser Delta, has not been updated in decades. I explore bedform distributions in the lower Fraser River which reveals dunes characterized by low sand supply to the bed in the main channel which supplies the delta. Repeat measurements of topography indicate that bed elevation has declined over the past 70 years, explaining why low sand supply dunes developed. To better understand the ongoing changes to the lower Fraser River and Delta, I examined changes in sediment delivery to the delta channels from changes in upstream sediment supply and bed topography, updating the contemporary sediment budget. The results indicate sediment delivery to the Fraser Delta has declined through time leading to a deficiency in bed material sediment needed to replenish the delta channels.

Keywords: Sediment budget; Sediment management; Sand-bedded rivers; Dunes; Fraser River

Acknowledgements

I would like to start off by thanking my supervisor Dr. Jeremy Venditti. It has been a pleasure working with you and the incredible team of researchers that you have assembled. Your hands off approach to supervising students allowed me the space to be creative and think for myself.

I also want to extend a big thanks to Dr. Ryan Bradley for being playing a key role in my journey from the beginning. Throughout the highs and lows, Ryan reassured me that a lot of the feelings I was experiencing were normal. Luckily, Ryan was very patient and persistent with his suggestions throughout the journey whether that was related to science or fishing. I would also like to extend a big thank you to the geomorphology crew at Northwest Hydraulic Consultants (Ryan, Ashley, Dave, Derek, Andrew, Joe, and more) it was a pleasure having the opportunity to work and collaborate with you all.

To the River Dynamics Laboratory graduate students (Max, Morgan, Kyle, Tingan) and the BCSRIF post-doc's (Erin, Aaron, Matteo, Jeff, Julia, Evan) thanks for all of the advice and support throughout this journey. It has truly been a pleasure being surrounded by such an amazing group full of inspiration and wisdom. Also, to the undergraduate research assistants who assisted me (Sonia, Laurie, Lianna), you all rock.

To my friends outside of the academic setting thank you for going on fun adventures with me exploring the beautiful backyard that we have here in British Columbia. The time spent outside of the office in nature is what has kept me grounded throughout this process and without the ability to 'recharge my batteries' I am not sure I would have been able to complete this journey with as full of a heart. I would also like to extend a special thanks to Max it has been a pleasure working and recreating in the mountains with you. Your unique character and your passion for science and the mountains is contagious and I hope you continue inspiring people.

Lastly, I would like to thank my family back in New York who provided support for me throughout the journey. It is hard to summarize how grateful I am in a few words. I miss you all very much.

Table of Contents

List of Tables

List of Figures

List of Acronyms

$\overline{\Delta\eta}$	change in average centerline bed elevation
ΔV_{chan}	change in sediment storage
C_{ss-BM}	concentration of suspended bed material
Q_{BM}	annual total bed material flux
Q_{daily}	daily discharge
Q_{ss-BM}	suspended bed material flux
Q_{ss-WL}	wash load flux
Q_{ss-tot}	total suspended sediment flux
$V_{chan-delta}$	change in sediment storage in the Fraser Delta channels
V_{dredge}	volume of sediment extractions
V_{in}	sediment supply
V_{in-h}	historical sediment supply
V_{in-b}	blended sediment supply
V_{in-c}	contemporary sediment supply
$V_{in-delta}$	sediment supply to the delta channels
V_{out}	sediment output
V_{spoil}	volume of dredged sediment disposed of at sea
2D	two-dimensional dunes
2Dc	high complexity (complex), two-dimensional dunes
2Ds	low complexity (simple), two-dimensional dunes
3D	three-dimensional dunes
BCF	bias correction factor
Brchn	barchan dunes
CGVD28	Canadian Geodetic Vertical Datum 1928
CHS	Canadian Hydrographic Service
ECCC	Environment and Climate Change Canada
Fb	flat bed
GiT	dunes with gaps in the trough
GST	gravel-sand transition

H	dune height
h	flow depth
H/h	dune height-depth scaling relation
L	dune length
L/H	dune aspect ratio
L/h	dune length-depth scaling relation
MBES	multi beam echosounder
NbD	near-bank deposits
PWC	Public Works Canada
Q	Discharge
RK	river kilometer upstream of the ocean
SB	single beam echosounder
S_f	slipface angle
S_t	transverse bed slope
Wd	wake deposit
WSC	Water Survey of Canada
WSL	Water surface level
Z	bed elevation

Chapter 1. Spatial Variability of Bedforms in a Large Lowland River

Abstract

Current understanding of bedforms in sand-bedded rivers is based on flume experiments, measurements of local bedform fields in natural channels with limited spatial extents, and stratigraphic interpretations of fluvial deposits. While it is widely recognized that bedform fields are comprised of a spectrum of different-sized bedforms that are hierarchical in nature, investigations of bedform spatial variability in large lowland rivers are lacking. Here, I examine bed topography and bedforms in a 35-km long reach of the sand-bedded lower Fraser River, British Columbia. I categorize bed features as 1) continuous (2D-complex, 2D-simple and superimposed dunes), 2) discontinuous (dune with gaps in the troughs, isolated and barchan dunes), 3) unclassifiable (features smaller than the resolution of the surveys; ~0.5 m), and 4) non-bedforms (flatbed surfaces, wake-deposits, and near-bank deposits). I find ~63% of the bed is composed of continuous dunes (2D-complex: 55%; 2D-Simple: 8%), while discontinuous dunes represent ~13% of the bed surface. A substantial portion of the bed (~21%) is composed of flat bed or near-bank deposits. There is spatial coherence to bedform distributions. The largest bedforms are low complexity 2D dunes, which occur on the sloping edge of lateral bars, with high complexity 2D dunes in the thalweg and flat bed or small bedforms on bar tops. I find that bedform fields in large lowland sand-bedded rivers are not ubiquitous or as spatially uniform as in small-scale laboratory channels. In large rivers, the size, scale, and type of bedforms depend on the location in the channel. Reports of single-transect surveys through bedforms fields or spatially resolved surveys of limited areas should be treated as local samples only and may not be representative of bed roughness in large sand bed rivers.

1.1. Introduction

In sand bedded rivers, bedforms have a wide range of sizes and morphologies. Bedforms are also an important source of flow resistance and sedimentary structures representative of bedforms can be preserved in the rock record which have been used to interpret past environments. Observations of bedforms are typically limited to

experiments in flumes and local bedform fields in rivers. Studies often rely on single-transect surveys through a bedform field or spatially resolved surveys of limited areas (e.g., Kostaschuk & Church, 1993; Kostaschuk & Villard, 1996; Parsons et al., 2005; Nittrouer et al., 2008; Bradley et al., 2013; Almedia et al., 2016; Hendershot et al., 2016, 2018; Cisneros et al., 2020; Bradley & Venditti, 2021; Ma et al., 2022). Field surveyed bedform fields are often selected for study because the spatial distribution of bedform type is uniform and they often have the largest features in the channel. Few observations of bedform spatial variability and the distribution of bedforms in large lowland rivers have been made, in part because of a paucity of observations that cover long reaches of rivers. However, recent technological advancements have increased surveying resolution and efficiency creating the opportunity for more detailed observations of bedform distribution in natural river channels.

It has been rarely acknowledged that bedform geometry and presence is not spatially uniform in natural sand bedded rivers which presents challenges for understanding of river systems and interpretations of past environments. Studies documenting the spatial distribution of bedform type are limited in natural river channels, but there are some notable exceptions. For example, Jackson (1975) documented the variation in dune size through a meander bend in the Illinois River. At low flows, they observed a plane bed through the thalweg and small dunes on the surface of the point bar with the largest dunes on the point bar slope. At high flows, the distribution was observed to be similar with dunes developing in the thalweg. Other local observations of dunes and sedimentary deposits in meandering channels have shown that there is substantial variability of the types of bedforms found on point bars. Some have found dunes with curved crestlines are the dominant bedform type on point bars (e.g., Jackson, 1975; Bridge & Jarvis, 1982; Bridge, 2003) while others have found large straight crested dunes (“transverse bars”), ripples, and upper-stage plane bed on meander point bars (e.g., Levey, 1978; Miall, 1996; Bridge, 2003). Between meander bends, straight sections in river channels have been observed to be composed of dunes including straight-crested dunes and straight to sinuous-crested dunes (Levey, 1978; Miall, 1996). In straight channel flume experiments, the largest dunes are found mid-channel (Stein, 1965), a characteristic also observed in straight natural channels that have lower stage plane beds or ripples on the channel margins (e.g. Jackson, 1975; Allen, 1982). Wu et al. (2021) found that in comparison to straight sections, dunes have

been observed to be larger in meander bends, which may be the result of varied flow velocity.

This spatial and flow stage dependent variation in bedforms in river reaches is problematic for hydrodynamic modelling because one flow resistance coefficient is used. Local roughness is widely thought to be a function of bedform type and size, yet field observations have not shown a strong relation between reach-scale flow resistance and bedform morphology (e.g., de Lange et al., 2021).

The spatial variation in bedforms is also problematic for interpretation of fluvial strata (e.g., cross-stratification, plane bed lamination) preserved in the rock record. Lateral accretion and point bar models for meandering rivers are partly based on variation in bedform type (Allen, 1965, 1970, 1982, 1985; Vishner, 1965; Bridge & Jarvis, 1982; Miall, 1996), but the models are based on assemblages of bedforms that appear to vary between studies and with flow stage. For example, depositional point bar models are typically characterized by lower flow regime bedforms including small ripples and dunes while the thalweg is composed of upper stage plane beds with degrading beds (Allen, 1963b; Miall, 1996). This bedform assemblage might exist at some sites, but is not universal (e.g. Jackson, 1975; Bridge & Jarvis, 1982; Allen, 1985).

More recent investigations of bedforms have used multibeam echo sounding which permits an unprecedented spatial resolution of bedforms, but studies often focus on limited spatial areas that are mapped repeatedly (e.g., Hendershot et al., 2016, 2018; Bradley & Venditti, 2021; Ma et al., 2022) or transects drawn through spatially resolved data (Wu et al., 2021; Prokocki et al., 2022). These investigations have led to important insights into the spatial variation in bedforms during dune growth and decay over tide cycles (e.g., Villard & Church, 2003; Bradley et al., 2013; Hendershot et al., 2016, 2018) or annual hydrographs (Bradley & Venditti, 2021). Multibeam echo sounding of lowland rivers has revealed a complex sequence of bedforms that arise from low sand supply to the bed (Venditti et al., 2019), confirming a sequence initially observed in flume experiments (Kleinhans et al., 2002). As upstream sediment supply and transport stage increase the following pattern of sandy bedforms develops successively over an immobile gravel bed: (i) sand ribbons; (ii) barchan-shaped dunes; and (iii) channel spanning dunes. Studies of transects through spatially distributed bed maps have shown some of the fundamental associations between grain-size, flow conditions and bedform

type and dimensions through the fluvial-tidal zone (e.g., Wu et al., 2021; Prokocki et al., 2022). These studies highlight the variation in bedform size and dimension, but the spatial resolution offered by the measurements are lost.

Our current understanding of sandy bedforms is limited to observations in localized reaches of natural channels, controlled laboratory settings and stratigraphic interpretations of sedimentary structures in rock outcrops. Bed configurations of sand-bedded channels have been observed (e.g., flumes, natural channels) and inferred (e.g., rock outcrops), but a detailed analysis of extended reaches in a modern channel is lacking. Here, I examine bed topography derived from multi-beam echosounder surveys during low flow conditions on a 35-km segment of the sand-bedded lower Fraser River. Bedforms present on the riverbed were identified and classified to highlight spatial variability in bedform type, morphology, and size. The fundamental question I address here is: Are bedforms in the Fraser River spatially uniform or variable? I examine (i) the variability in bedforms in the Fraser River, ii) whether bedforms follow patterns expected for meandering rivers; (iii) whether the distribution of bedforms is linked to coherent variation in the channel and grain size.

1.2. Methods

1.2.1. Field Site

The Fraser River drains ~232,000 km^2 of British Columbia, Canada. Discharge is snowmelt dominated with a prolonged period of high flow generally occurring from late May to early July before receding in August and September (Figure 1-1A). Flowing through a 375-km sequence of bedrock canyons, the Fraser River emerges as an alluvial channel near Hope, British Columbia at RK 185 (RK is river kilometers upstream of the river mouth at Sand Heads) (Figure 1-1B). At Hope (RK 167) a continuous record of discharge (Q) shows the mean annual Q from 1992 to 2021 was 2,750 $m^3 s^{-1}$ and the mean annual flood Q is 8,620 $m^3 s^{-1}$ with a recorded peak Q of 15,200 $m^3 s^{-1}$ in 1948 (Ham & Church, 2012). Downstream of Hope (RK 167) the alluvial channel emerges as an anabranching gravel bed channel that persists to ~RK 100.5 where a change in river gradient and washload deposition causes a gravel-sand transition (GST) (Venditti & Church, 2014) (Figure 1-2). Close to the gravel front, the bed is a mix of sand, bimodal

sand-gravel, and gravel (Venditti et al., 2019) to Mission, British Columbia (RK 85), the upstream extent of the lower Fraser River (Figure 1-2).

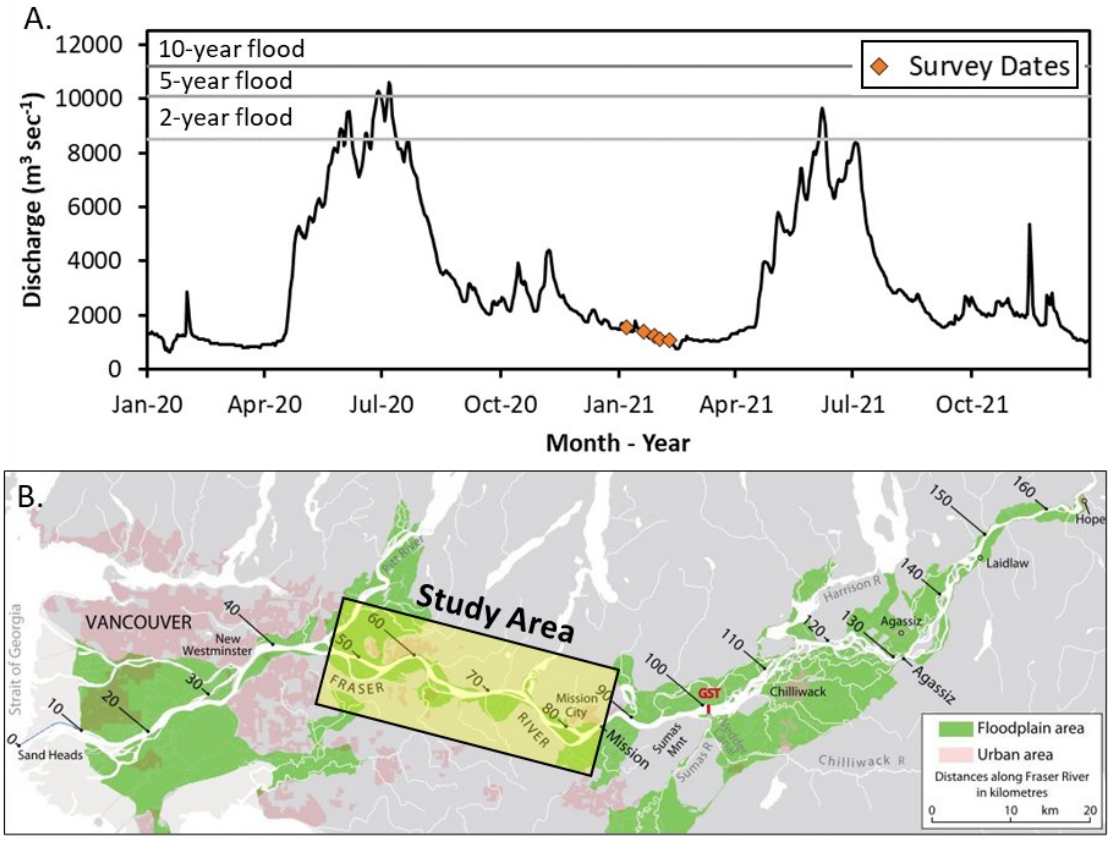

Figure 1-1. (A) 2020 and 2021 hydrograph for Hope, British Columbia (WSC Gauge 8MF005; RK 167) with Public Service and Procurement Canada (PSPC) bed topography survey dates plotted. (B) Map of the lower Fraser River, British Columbia. Modified from Venditti & Church (2014).

The presence of gravel diminishes, and the bed is assumed to be composed of sand downstream of Mission (RK 85), although this assumption is based on sparse bed sampling (Venditti & Church, 2014) (Figure 1-2). The mean annual Q at Mission from 1983 to 2013, was 3,183 $m^3 s^{-1}$ and the mean annual flood was 9,534 $m^3 s^{-1}$ (Haught et al., 2017). Downstream of Mission, the lower Fraser River is dominantly a single thread, sand-bed channel with bends that have back channels in the apices. The river is not actively meandering, because most of the water is carried through the inside of bends rather than the apices (Venditti & Church, 2014). Engineering controls (e.g., riprap, dikes, jetties, etc.) have also contributed to fixing the current position of the lower Fraser River. In the sand bed reach, sand is carried as suspended bed material load and

bedload in the form of migrating dunes (Venditti et al., 2019). The bed material-wash load division is 0.177 mm (McLean et al., 1999; Attard et al., 2014) and the sand bed has a median size of ~0.385 mm (Venditti & Church, 2014). A tidal influence is present downstream of Mission ranging from a few a centimeters during the freshet to > 1 m during the winter tides (Attard et al., 2014). At New Westminster (RK 34), the river bifurcates forming the Fraser Delta (Figure 1-1B).

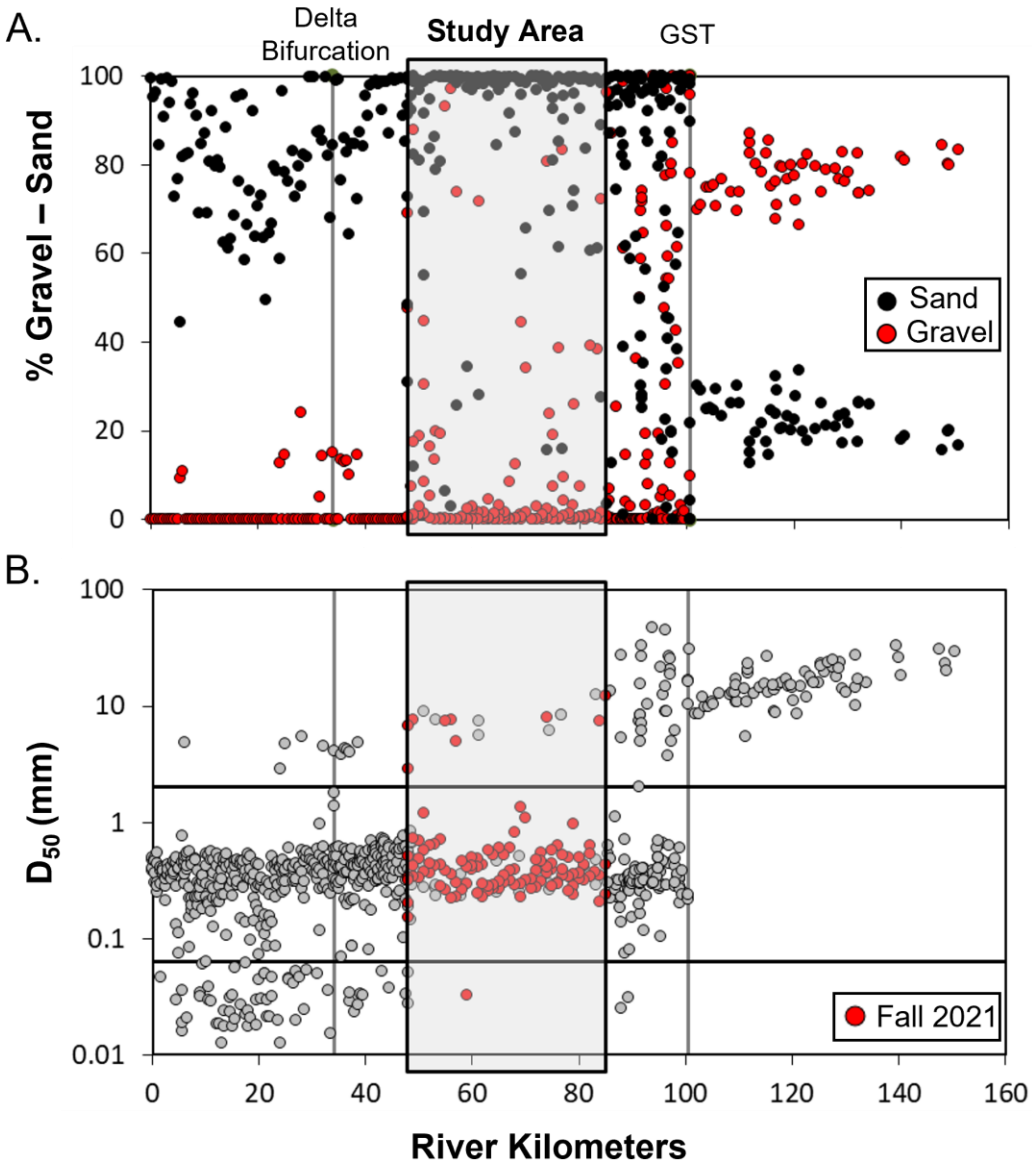

Figure 1-2. Downstream change in A) percent gravel and sand and B) median grain size (D_{50}) in the alluvial portion of the Fraser River from Hope, British Columbia (RK 167) to the mouth of the Fraser River at Sand Heads (RK 0). Previous grain-size data from: McLaren & Ren, 1995; Venditti & Church, 2014; McLean, 1990; Ham, 2005.

1.2.2. Observations

This study used multibeam echosounder (MBES) bed topography data from Mission (RK 85) to RK 47, downstream of Barnston Island before the confluence with the Pitt River. The bed topography data was collected and processed by the Public Service and Procurement Canada (PSPC) in 2021. A Kongsberg 2040C Dual with a Real Time Kinematic GNSS was used to collect bed topography data. Vessel heading, pitch, heave, and roll were measured with an Applanix POS MV inertial guidance system. Raw bed elevation data were processed to correct for tidal stage, pitch, heave, roll and sound velocity, and to remove spurious data points. Data were gridded at 0.5 m horizontal resolution with bed topography referenced to Canadian Geodetic Vertical Datum 1928 (CGVD28). The 2021 survey was conducted during low flow conditions following the 2020 freshet which had a peak flood discharge of 10,600 m^3 s^{-1} at Hope, British Columbia (Figure 1-1A). The spatial extent of the surveys included most of the main channel and portions of the side channels through RK 47 to 85 (Figure 1-3). Data were not collected from RK 74 to 71 by PSPC in the winter of 2021.

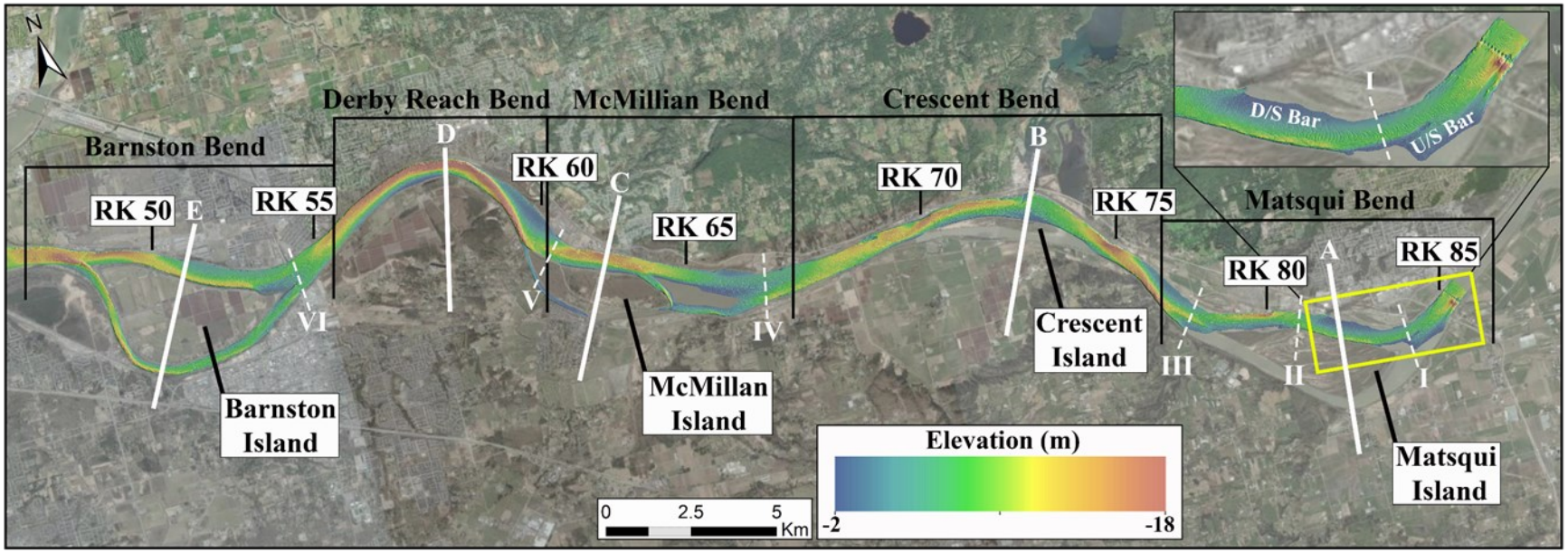

Figure 1-3. **Multibeam bed topography of the lower Fraser River (RK 85-47). The bathymetric data was collected during 2021 low flow conditions by PSPC. The white lines (A-E) represent primary meander bend apices (A: Matsqui Bend; B: Crescent Bend; C: McMillian Bend; D: Derby Reach Bend; E: Barnston Bend). The dashed white lines (I-VI) represent secondary bend apices. Bathymetry data from RK 74 to 71 were collected during 2020 high flows (>5,000 m^3 sec^{-1}) and included in this figure to provide a complete map of the riverbed surface. Since this data was collected in high flow conditions it was not included in analyses of the bed surface.**

Bed material samples were collected in the Fall of 2021 during low flow conditions to establish the spatial distribution of bed material grain-size (Figure 1-2). Samples were collected at approximately 25%, 50%, and 75% of the main channel width and in the middle of side channels every 1 RK. The samples were collected with a dredge sampler which was dragged along the riverbed until it was filled with sediment from where it initially contacts the bed surface, and from the bed surface which it is dragged along. As a result, the ~1 kg samples are comprised of surface and shallow subsurface material, which is sufficient to meet the stringent sediment sampling procedures proposed by Church et. al (1987). Some samples contained individual gravel clasts, which are underrepresented in the sample. Therefore, some caution is needed in characterizing coarse fraction sizes. Additional target sampling was conducted in the Spring of 2022 to examine the composition of bed material in discontinuous dune fields. To guide the target sampling a grid of proposed sampling locations was drawn over a discontinuous bedform field found upstream of Matsqui Island. In addition to the sampling grid, an echosounder was used in the field to confirm the presence of discontinuous bedforms.

1.2.3. Bedform classification

A bedform classification scheme was developed that uses existing terminology and groupings (e.g., Ashley, 1990; Kleinhans et al., 2002; Venditti et al., 2005b, 2019; Hendershot et al., 2016, 2018) to categorize the bed into several general categories including: (i) continuous dunes; (ii) discontinuous dunes; (iii) unclassifiable bedforms, and iv) non-bedforms; (Figure 1-4). Continuous dunes have crestlines that are laterally continuous and troughs (local minima) immediately downstream of crests (local maxima), without flatbed sections between them. Continuous dunes were divided into: (i) two-dimensional (2D) dunes; (ii) three-dimensional (3D) dunes; (iii) superimposed dunes where multiple scales of bedforms are present. Two-dimensional dunes display regular spacing, heights and lengths with straight or slightly sinuous crestlines oriented perpendicular to mean flow lines (Venditti et al., 2005b). Three-dimensional dunes generally have crestlines whose length is 1.4 times the distance between the ends of the crestline across the channel and have irregular spacing, heights and lengths with highly sinuous or discontinuous crestlines (Venditti et al., 2005b). True 3D dunes are rare in the study reach, but there are two populations of 2D dunes that can be divided based on the

complexity of the crestlines. High complexity 2D dunes (2Dc) have numerous bifurcations of the crestlines while low complexity (or simple) 2D dunes (2Ds) are generally larger and have straight crestlines. Superimposed dunes are generally characterized by smaller dunes migrating overtop of larger dunes (Venditti et al., 2005a; Galeazzi et al., 2018; Zomer et al., 2021).

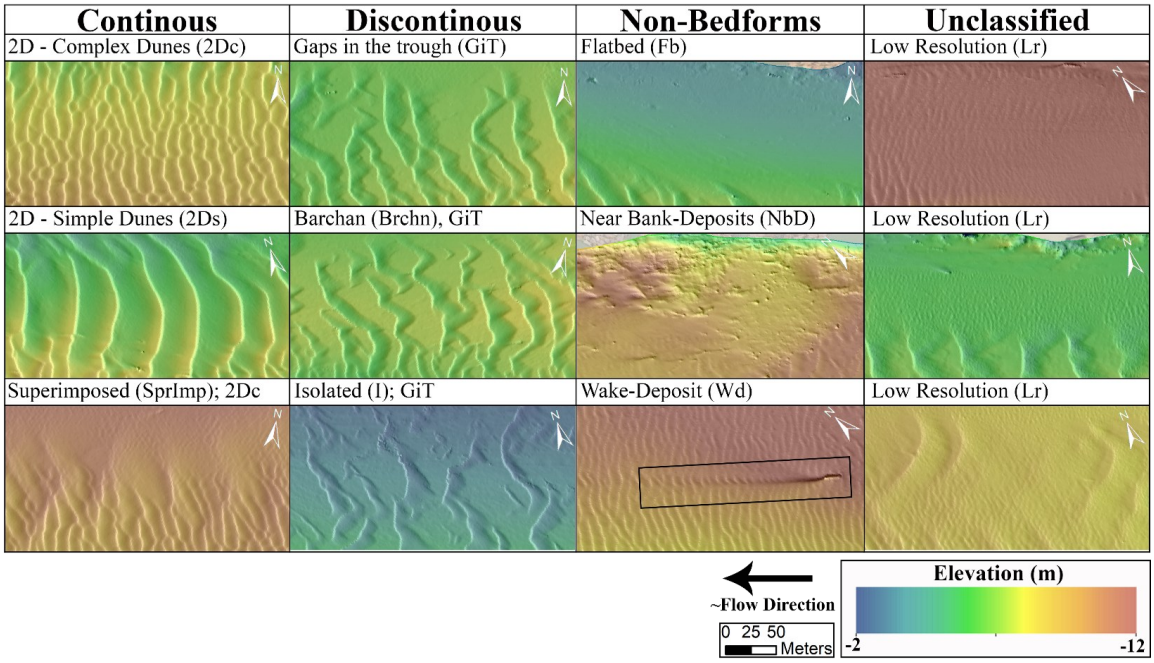

Figure 1-4. Bedform classification scheme: 1) continuous dunes (2D-complex, 2D-simple, superimposed); 2) discontinuous dunes (barchan, isolated, dunes with gaps in the trough); 3) non-bedforms (flat bed, near bank-deposits, wake-deposits); 4) unclassifiable (low resolution bedforms at or near the resolution of the bathymetry; ~0.5m).

Discontinuous dunes are typically associated with a localized sand supply limitation. Sand supply may be abundant from upstream, but the dynamics of how it is carried as bedload, suspended bed material load, or washload, limit its availability to build bedforms (Venditti et al., 2019). Discontinuous dunes may be categorized as: (i) barchan dunes; (ii) isolated bedforms; and (iii) dunes with gaps in the trough. Barchan dunes have crestlines that have lateral termination and whose crestlines bow in the downstream direction (Venditti et al., 2019). Dunes with gaps in the troughs have flat bed between crests and troughs. Isolated dunes are individual dunes without any other bedforms in close proximity and typically appear on a nearly flat bed. There is a sequence of sand dunes that occur with increasing sand supply to the bed that includes

isolated dunes, barchan dunes and dunes with gaps in their troughs (Kleinhans et al., 2002; Venditti et al., 2019). Gaps in the troughs of discontinuous dunes may be caused by an immobile layer consisting of material such as gravel, coarse sand or clay that forms the bed that the dunes migrate over. Additional target sampling was conducted to further understand the grain-sizes associated with discontinuous dunes.

Some patches of the bed are unclassifiable when there are bedforms present because their size is at or below the spatial resolution of the bathymetry (H ≈ 0.5 m). The unclassifiable bed has a hummocky, textured appearance, but topographic profiles do not have sufficient data density to characterize bedform morphology. Some patches of the bed do not have bedforms present which I refer to as non-bedforms because the bed features lack specific geometries associated with bedforms. Non-bedforms include (i) near-bank deposits, (ii) wake-deposits downstream of an obstacle, (iii) flatbed surfaces. Near-bank deposits are commonly found near the edges of channels and appear to be composed of immobile materials (e.g., bedrock, gravel, glacial deposits, riprap, large woody debris, etc.). Wake deposits are streamlined, topographic highs found behind bed features such as bridge supports, gravel, or other debris found on the riverbed and that appear to be sculpted features. Flat beds may be either lower regime flat beds or upper regime flat beds although they may also be immobile clay or gravel surfaces. In comparison to unclassifiable bed features, flat beds have a low rugosity.

The riverbed was classified by manually drawing polygons around the different bed types shown in Figure 1-4. The survey was divided spatially into five bends (A-E): Matsqui Bend, Crescent Bend, McMillian Bend, Derby Reach Bend, and Barnston Bend (Figure 1-3). The extent of each bend was defined as segments of the channel that extend from the upstream and downstream meander apex to meander apex. There is also a series of six secondary bends (I-VI) that exist below the scale of the five major bends. The secondary bends have a lower radius of curvature in comparison to the primary bends and are caused by the development of lateral bar sequences through the primary bends (Figure 1-3).

Dune characteristics in two dimensions were also examined along three along stream profiles stretching across 25% (Profile-25), 50% (Profile-50), and 75% (Profile-75) of the main channel width of the survey reach. Dune height (H), length (L), and slip

face angle (S_f) were measured along the profiles. Dune length-depth (L/h), heigh-depth (H/h) and aspect ratio (L/H) were also measured. Flow depth (h) was defined as:

$$h = WSL - Z \quad \text{Equation 1-1}$$

where WSL is water surface level and Z is bed elevation. Bed elevations were derived from the along stream profiles of Z extracted from the 2021 bathymetry. WSL was calculated by interpolating the low water surface between the WSC Mission gauge (08MH024; RK 85), WSC Whonnock gauge (08MH044; RK 70), and the CHS New Westminster gauge (RK 35) for the bed topography survey dates. Additionally, 2Dc and 2Ds dune H and L were measured along target profiles of bed elevation to compare dune dimensions. Target profiles were drawn through segments of 2Dc and 2Ds dune fields in meander bend and straight sections of the channel.

In order to explore potential controls on bedform type and size through the reach, we calculated reach-scale morphological metrics to compare against dune geometry and scaling relation patterns observed. Channel parameters including curvature, transverse bed slope (S_t), and depth excess (h_{ex}) were also measured to assess how different aspects of channel geometry may be related to the distribution of bedform types. Curvature is defined as the inverse of the bend radius (r) (de Ruijsscher et al., 2020). Transverse bed slope (S_t) is defined as the slope between the two edges bounding the river channel longitudinally, discretized in parts of 100m. Depth excess (h_{ex}) is defined as

$$h_{ex} = \sin(r)\,(h_{max}/h - 1) \quad \text{Equation 1-2}$$

where h is the regional mean depth of a discretized section of 500 m long and h_{max} the local maximum depth found in the 500 m long section (Vermeulen et al., 2014).

1.3. Results

1.3.1. Reach Topography

The study reach consists of five primary bends in the river, four of which have an island with a back channel in the apex (Figure 1-3). There are also a series of secondary bends in the river which are oriented around the main channel and generally have a lower radius of curvature (Figure 1-3). A series of alternating bars throughout the study reach coincide with the secondary bends and occur in a sequence. Generally, a bar is

found on the outer bank upstream of a secondary bend and another bar is found on the inner bank downstream of a secondary bend. For example, upstream of secondary bend apex I, there is a bar on the outside bend of the main channel where the main channel bifurcates forming the side channel at the upstream end of Matsqui Island (Figure 1-3). Downstream of secondary bend apex I, another bar is found on the inside bank of the channel (Figure 1-3). In this commonly observed sequence, both bars thin towards the apex of the secondary bend and increase in size as they move away from the apex (Figure 1-3).

1.3.2. Grain Size

The main channel was primarily composed of sand (88.6%) with minor components of gravel (10.1%) and silt/clay (1.20%) (Figure 1-2). There is no downstream fining in the bed material grain size (Figure 1-2b), however, there are gravel deposits in several locations throughout the study reach (Figure 1-2a). Grain-size appears to vary coherently with channel morphology (Figure 1-5a). Generally, coarser bed material was observed in the thalweg of the channel with finer material on the bar tops and bar slopes (Figure 1-5b). Bar tops are defined as the shallow platform on the point bar and the bar slope is the sloping transition from the bar top to the thalweg. For example, between RK 55 and RK 57 there is cross-stream fining with gravel in the thalweg with a mode of 8.00 mm, sand on the bar slope with a mode of 0.250 mm, and finer sand on the bar top with a mode of 177 μm (Figure 1-6b). There are also examples of cross-stream coarsening. For instance, at RK 78, the downstream end of Matsqui Island, the D_{50} in the thalweg is 258 μm, 341 μm on the bar slope and 493 μm on the downstream end of a lateral bar (Figure 1-6c). In some locations, the coarser bed material occurs on the bar slope and bar top instead of in the thalweg. For example, at RK 82 on the slope of a lateral bar, the bed was 39% gravel with a D50 of 630 μm with finer sand on the bar top and thalweg (Figure 1-6d). There are some patches of mixed gravel and sand on the bed such as, on the bar slope around ~RK 83.5 where discontinuous dunes have been observed. Here the bed sediment was bimodal with a sand mode of 0.250 mm and a gravel mode of 8.00 mm (Figure 1-6e).

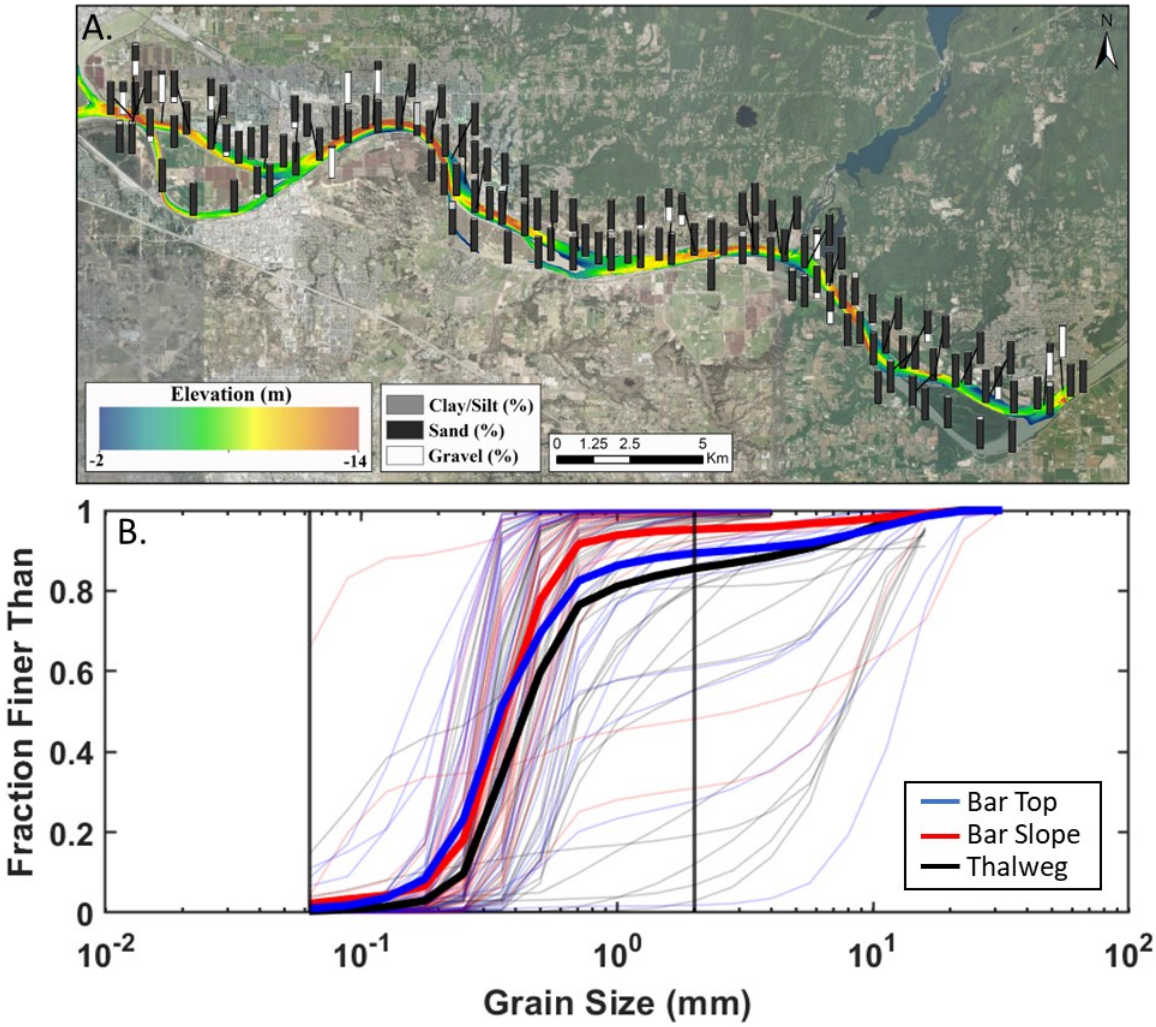

Figure 1-5. **(A) Distribution of bed material grain-size for the study reach (RK 85-RK 48). Sediment samples were collected in the fall of 2021 during low flow conditions (see Figure 1-1). (B) Grain-size distributions of bed material sediment samples for the main channel of the study reach. The vertical black lines delimit sand size.**

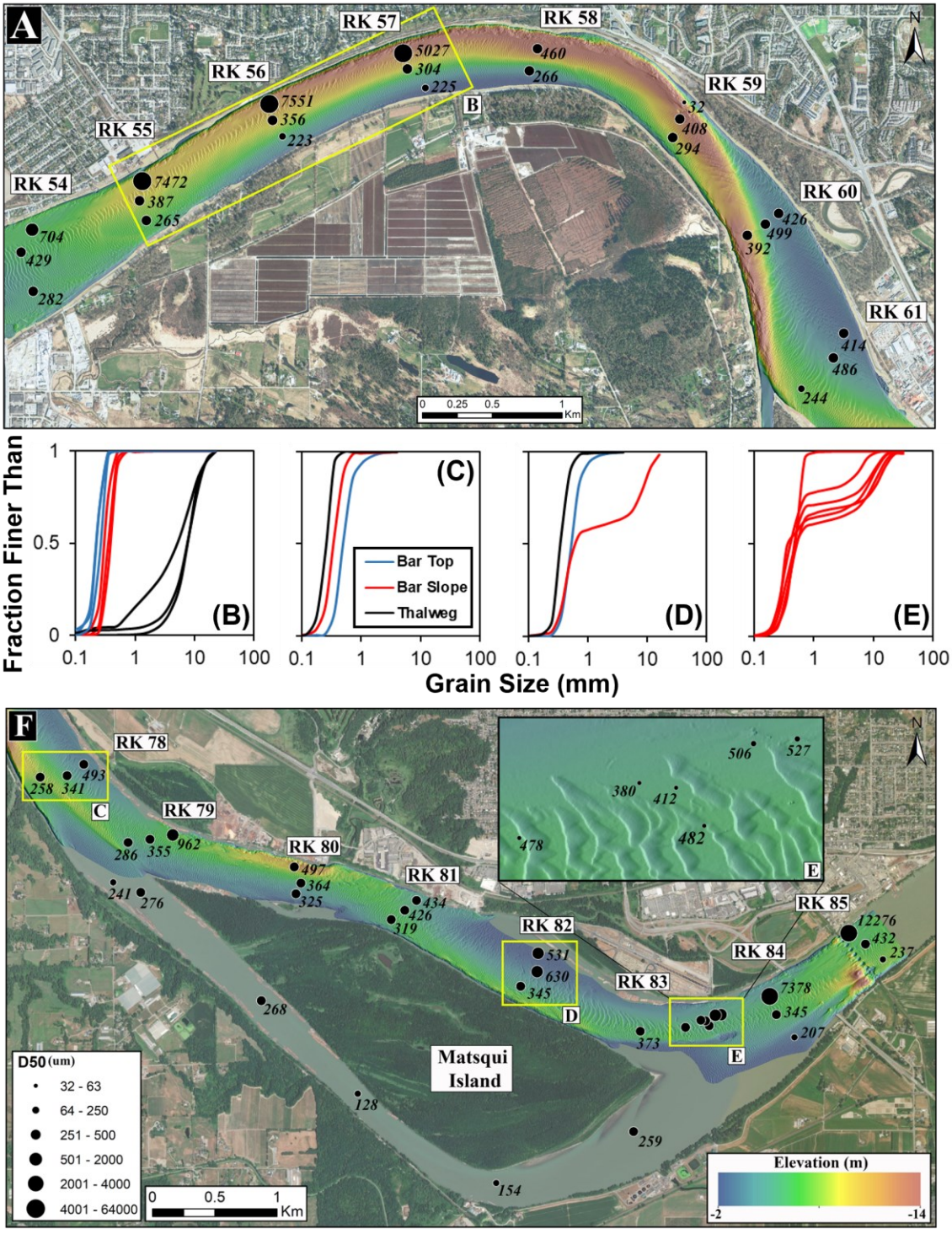

Figure 1-6. **Distribution of bed material grain-size from RK 61 to 54 (A) and RK 85 to 78 (F). The yellow boxes highlight areas with GSD curves shown and the location of target sampling: (B) RK 57 to 55; (C) RK 78; (D) RK 82; (E) target sampling (~RK 83.5). Bed material samples were not collected at the same time as the bed elevation data used to derive the bathymetry shown.**

1.3.3. Spatial distribution of bedforms types

There is substantial bedform spatial variability throughout the 35-km reach. Much of the variability exists at the local scale which is highlighted by a series of examples in Figure 1-7. At RK 61, there are discontinuous barchan (Brchn) dunes on the bar top, simple 2D (2Ds) dunes on the bar slope, complex 2D (2Dc) dunes in the thalweg, and near-bank deposits (NbD) on the edge of the channel (Figure 1-7a). Between RK 53 and 53.5 there are NbD, unclassifiable, low resolution (Lr) bedforms and a flatbed (Fb) on the bar top, discontinuous GiT dunes and 2Ds dunes on the bar slope, and 2Ds dunes in the thalweg (Figure 1-7b). Between RK 82.5 and 83.5, there are discontinuous GiT dunes and a Fb on the bar top, 2Ds and discontinuous GiT dunes on the bar slope, and 2Dc dunes in the thalweg and the south bank (Figure 1-7c). Between RK 67 and 68.5, there is a fairly typical sequence of bedforms with Fb/Lr bedforms on the bar top and discontinuous (GiT; Brchn) dunes on the bar slope which transition to 2Ds dunes and a 2Dc dune field in the thalweg (Figure 1-7d). The local examples presented here suggests that there are relatively consistent bedform patterns. These bedform patterns can be more clearly illustrated by isolating bars in channel bends and straight sections in between meander bends.

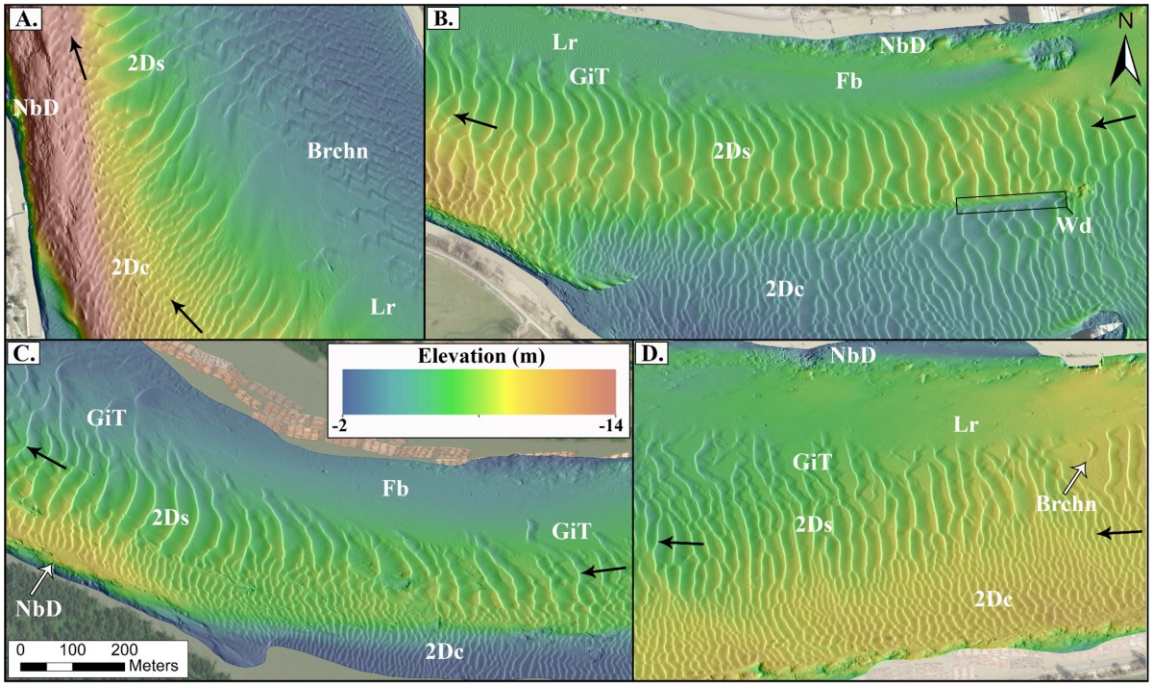

Figure 1-7. Spatial variability of bed features at the local scale on the lower Fraser River. (A): ~RK 61; (B): ~RK 53 to 53.5; (C): ~RK 82.5 to 83.5; (D): ~RK 67 to 68.5. The black arrows indicate the general flow direction.

In channel bends, cross-stream variation in bedform type is generally characterized by Lr bedforms, Fb, or discontinuous dunes on bar tops, large 2Ds dunes on the bar slope, and smaller 2Dc dunes, or flat bed in the thalweg of the channel (Figure 1-8). Bedform type varied on bar tops in the downstream direction with Fb/Lr dunes, discontinuous dunes (Brchn; GiT) and 2Dc dunes progressing from the upstream to the downstream end (Figure 1-8). This bar top sequence is consistent with increasing sand supply to the bed in a low sand supply environment (Kleinhans et al., 2002; Venditti et al., 2019). In some locations, the thalweg of the channel through a bend has discontinuous dunes or a flat bed, in addition to 2Dc dunes. There are some locations with low amplitude undulations in the thalweg that are suspected to be remnants of larger dunes that were cannibalized by smaller dunes during dune decay following higher flows (Bradley & Venditti, 2021).

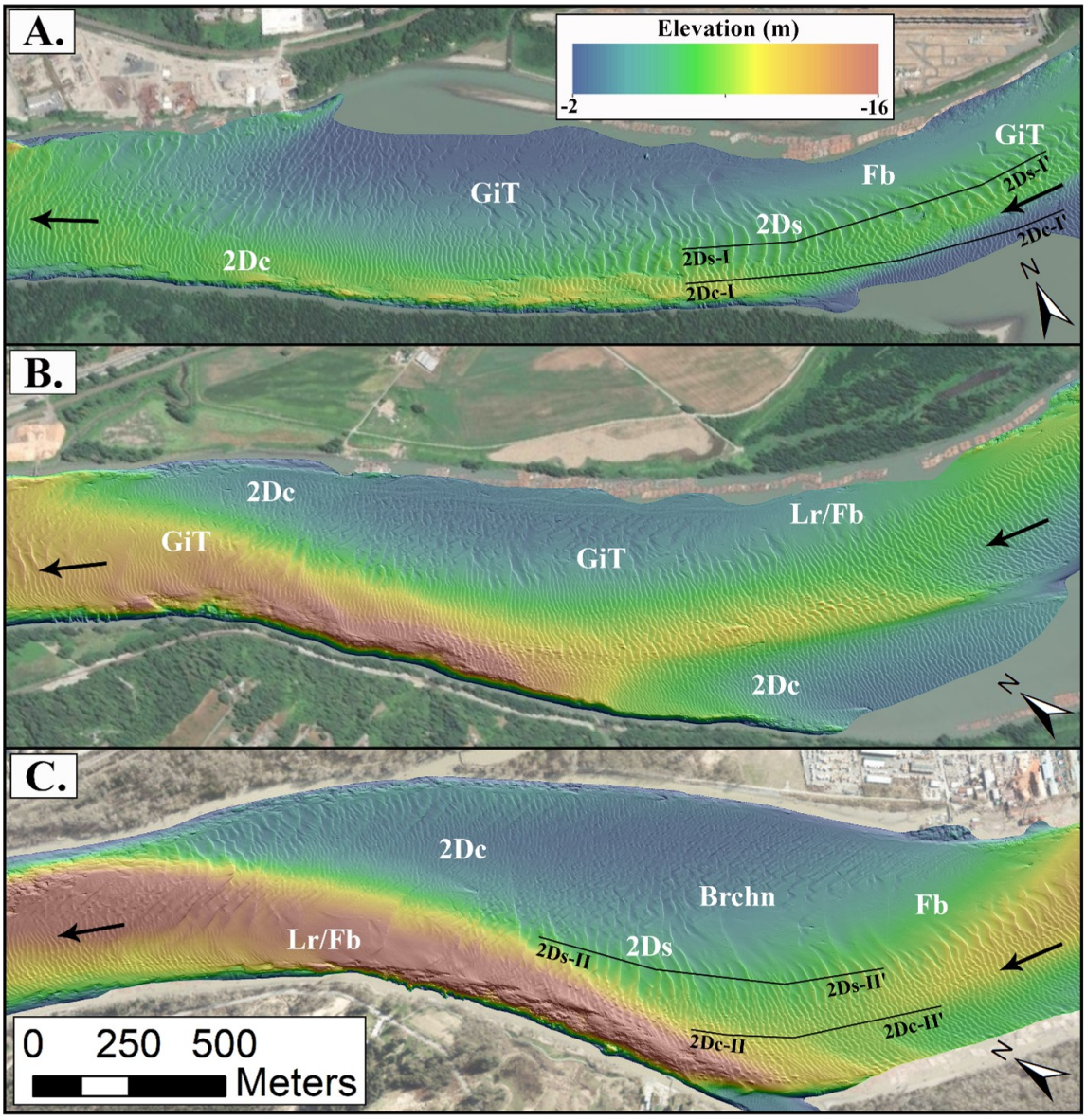

Figure 1-8. Bedform sequences through meander bends. (A) secondary meander bend I (~RK 84-81), inside edge bar downstream of the bend apex; (B) secondary meander bend III (~RK 79-76), inside edge bar downstream of the bend apex; (C) secondary meander bend V (~RK 62-59), inside edge bar downstream of the bend apex. The black arrows indicate the general flow direction. Black long profiles: 2D-I to 2D-I' and 2D-II to 2D-II' represent the profiles used to measure 2Ds and 2Dc bedform L and H found in Table 1-1.

In straight portions of the channel, between two bars, the cross-stream variation is generally characterized by Lr/Fb surfaces in the thalweg, with 2Ds dunes and 2Dc dunes adjacent to the thalweg (Figure 1-9). There is generally a sharp transition between Lr/Fb surfaces and the main bedform field ascending in bed elevation away

from the thalweg. Discontinuous dunes can be found at this contact (Figure 1-9). The cross-stream sequence of bedforms observed in straight sections generally continues in the along stream direction until there is a change in channel geometry (e.g., approaching a bend or island/back channel).

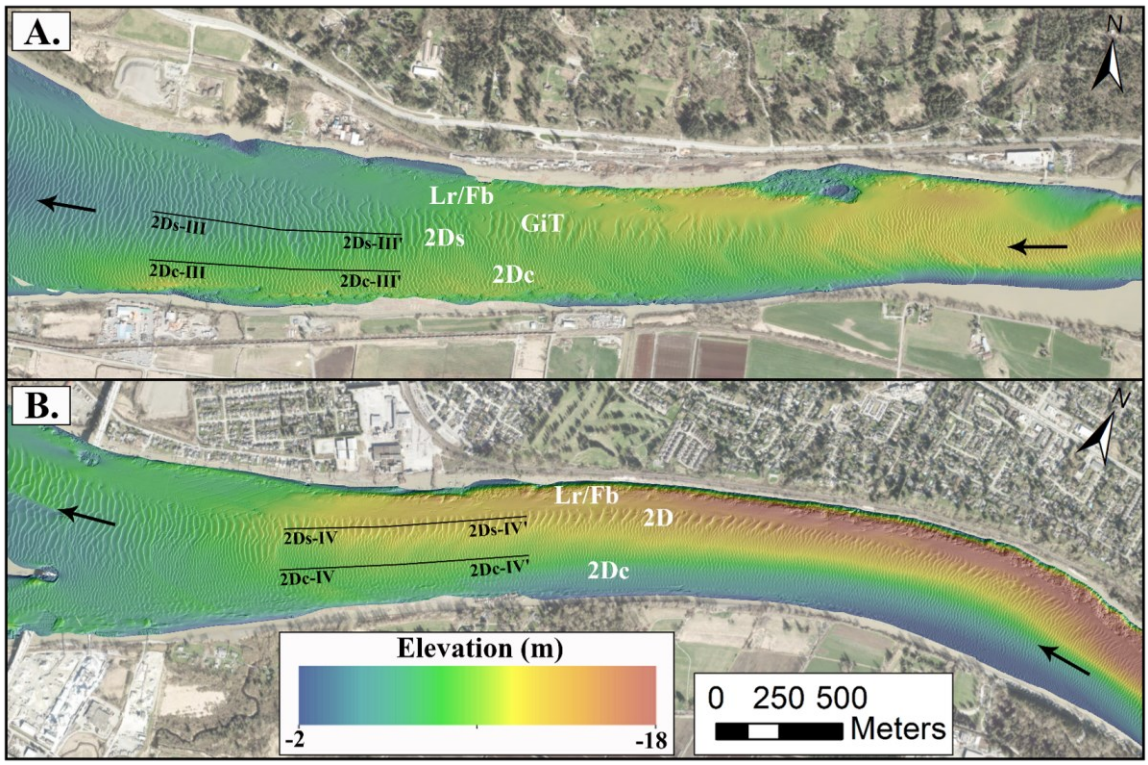

Figure 1-9. Bedform sequences through straight sections in the channel. (A) ~RK 71 to 66; (B) ~RK 58 to 54. The black arrows indicate the general flow direction. Black long profiles: 2D-III to 2D-III' and 2D-IV to 2D-IV' represent the profiles used to measure 2Ds and 2Dc bedform L and H found in Table 1-1.

There is substantial variation in bedform patterns throughout the study reach, but some consistent bedform sequences can be generalized. On bar tops, the following bedform sequence was commonly observed from the upstream to the downstream end: i) flat bed/low resolution bedforms; ii) dunes with gaps in the trough; iii) 2Dc dunes. On bar slopes 2Dc and 2Ds dunes were commonly observed. 2Ds dunes occur on the upstream end of the bar and 2Dc dunes typically occur on the downstream end of the bar. Discontinuous dunes were observed on bar slopes specifically upstream of a bend apex. In the thalweg, bedforms are generally 2Dc dunes although flatbed/low resolution bedforms and 2Ds dunes were observed in thalweg through straight sections between

bars. On the edge of the channel, non-bedforms and near-bank deposits are commonly observed.

The bed was spatially classified using a simplified scheme from that in Figure 1-4. Isolated dunes were grouped with discontinuous GiT dunes because isolated bedform fields were often composed of discontinuous GiT dunes. Superimposed dunes represented a small portion of the bed often occurring on the edge of 2Dc and 2Ds dune fields and were therefore not mapped. Non-bedforms, flat bed and near-bank deposits were grouped due to the close proximity of the features and wake-deposits were not included in classifications because they were often small and found within close proximity to the other bed classifications. A classified map reveals that the riverbed is comprised mainly of continuous 2Dc dunes (Figure 1-10), but a substantial portion of the channel bed is composed of discontinuous dunes with GiT and bed features that are not bedforms (Fb/NbD) (Figure 1-10).

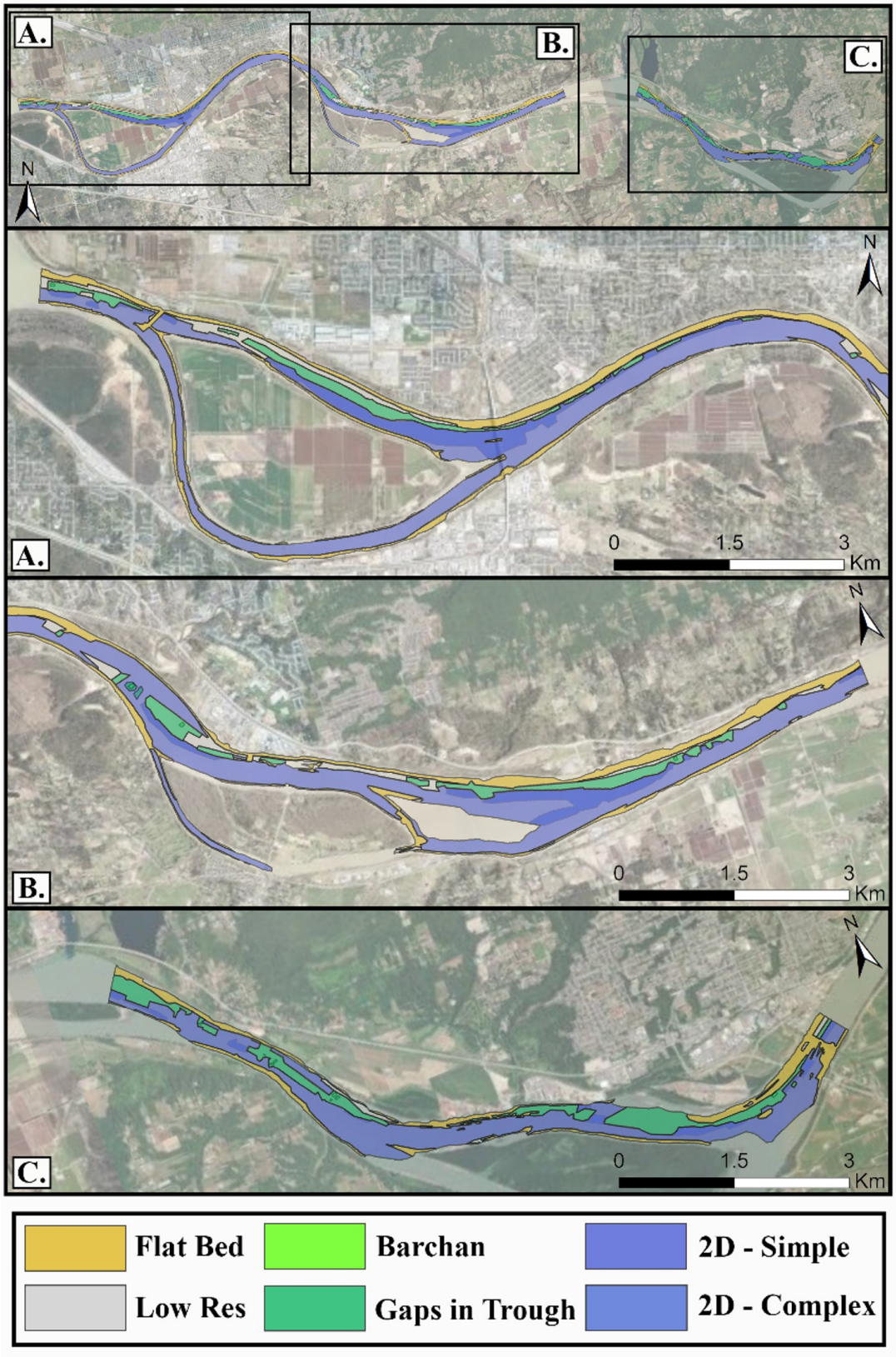

Figure 1-10. Classified polygon map of the lower Fraser River's bed features.

Continuous dunes mapped were classified as 2Dc or 2Ds features with 2Dc features dominating. The size of the 2Ds dunes differs from 2Dc features substantially with 2Ds dunes being twice the size of 2Dc dunes (Table 1-1). The mean H of 2Ds dunes is 1.06 m, while the mean H of 2Dc dunes is 0.465 m. The mean L of 2Ds dunes is 29.6 m, while the mean L of 2Dc dunes is 14.1 m.

Profile	H mean (m)	H SD (m)	L mean (m)	L SD (m)
2Ds-I to 2Ds-I'	1.17	0.28	31.01	5.95
2Dc-I to 2Dc-I'	0.50	0.13	14.62	2.10
2Ds-II to 2Ds-II'	0.93	0.25	32.98	9.72
2Dc-II to 2Dc-II'	0.49	0.18	14.89	3.08
2Ds-III to 2Ds-III'	0.99	0.17	24.89	5.20
2Dc-III to 2Dc-III'	0.44	0.11	12.88	2.17
2Ds-IV to 2Ds-IV'	1.15	0.30	29.44	6.31
2Dc-IV to 2Dc-IV'	0.43	0.14	13.82	2.51
2Ds - ALL	1.06	0.25	29.58	6.80
2Dc - ALL	0.47	0.14	14.05	2.46

Table 1-1. Dune H and L measurements of 2Ds and 2Dc dunes. Profile locations are shown in Figure 1-8 and Figure 1-9.

There is coherent spatial variation in bedform types throughout the study reach and on lateral bars. The classified bed surface in Figure 1-10 was dominated by continuous dunes which represented ~62% of the total classified area. Of the total classified area 8.4% was 2Ds and 54% was 2Dc, followed by flat bed/near-bank deposits (20%) and discontinuous dunes with gaps in the trough (12%) respectively (Figure 1-11a). Lateral bars were also primarily composed of continuous dunes representing ~43% of the lateral bar surfaces. Of the classified lateral bar area 0.15% was 2Ds and 43% was 2Dc, followed by discontinuous dunes with gaps in the trough (27%) and flat bed/near-bank deposits (22%) respectively (Figure 1-11b). Dunes with GiT were more common on bar tops in comparison to the entire classified bed surface which suggests a local low sand supply condition on bar top surfaces.

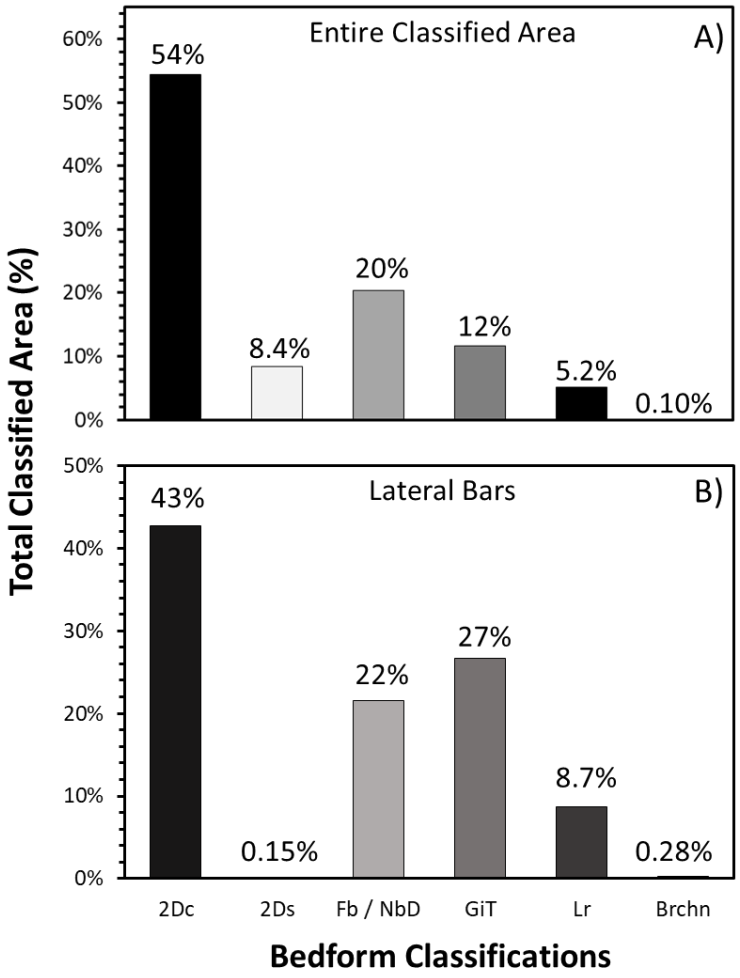

Figure 1-11. Spatial distribution percentages of bedforms for the entire classified area (A) and (B) lateral bars.

1.3.4. Spatial distribution of dune dimensions

There is no downstream trend in dune size and slipface angle (Figure 1-12). Dune H varied between 0.22 to 1.5 m with a median of 0.54 m and standard deviation of 0.30 m. Dune L varied between 8.0 to 54 m with a median of 16 m and standard deviation of 8.2 m. Dune H and L values from the data presented here fall into the range of the global dataset of dune field data (Bradley & Venditti, 2017). S_f angle varied between 4.6° to 28° with a median of 13.1° and a standard deviation of 5.1°, indicating low angle dunes (Sf angle <24°), which are characteristic of deep rivers (Kostaschuk & Venditti, 2019; Venditti & Bradley, 2022).

Dune H/h varied from 0.011 to 2.5 with a median of 0.064 and standard deviation of 0.040. Dune L/h varied from 0.45 to 8.2 with a median of 1.9 and standard deviation of 1.3. Dune steepness (L/H) varied between 32 to 59 with a median of 30 and a standard deviation of 7.6. While these metrics of dune geometry vary with transport stage (Bradley and Venditti, 2019; Venditti and Bradley (2022), our observations are consistent with the Bradley & Venditti (2017) global database of dune field data where the median H/h is 0.146 (standard deviation, $\sigma = 0.235$), the median L/h is 5.14 ($\sigma = 5.48$) and the median L/H is 34.4 ($\sigma = 47.1$). Here, dune geometry values are either larger or smaller, but within one standard deviation of the global database. The wide range of dune scaling relations (H/h, L/h, H/L) indicates that dunes do not increase with depth, however, there is coherent variation in dune size linked to the secondary bends in the channel. Both H/h and L/h generally peak after a secondary bend in the channel (Figure 1-12) which coincides with the presence of a lateral bar (Figure 1-3). This trend in the data is less apparent in the L/H and S_f measurements.

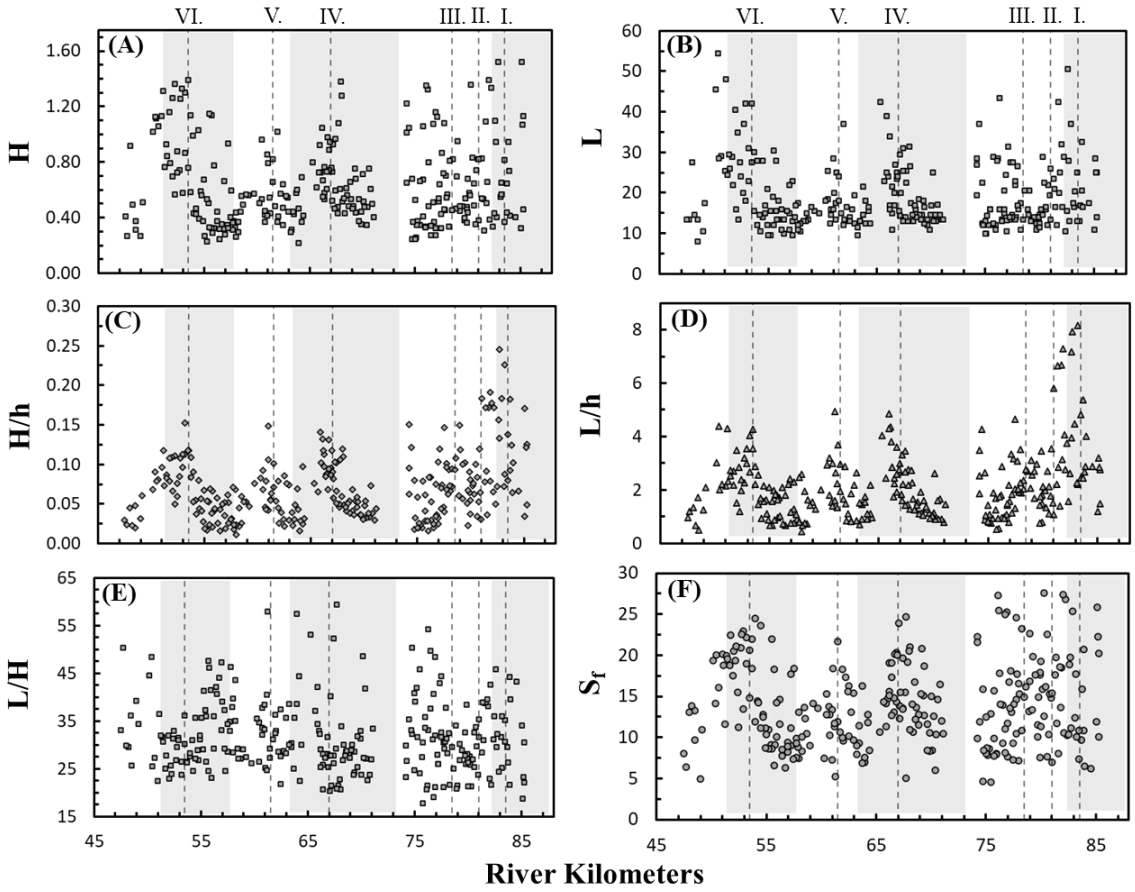

Figure 1-12. Downstream change in dune: (A) height (H); (B) length (L); (C) height-depth scaling (H/h); (D) length-depth scaling (L/h); (E) aspect ratio (L/H); (F) slipface angle (S_f). Bedform measurements are derived from three profiles (25%, 50%, and 75% of the channel width) for the 2021 survey year. Profile-25 (n=55); Profile-50 (n=117); Profile-75 (n=109). The dashed vertical lines represent scondary bends apices (I – VI) and the alteration between white and light gray shading represents the bounds of the primary bends.

A series of topographic profiles through secondary bend III (Figure 1-3) highlights how dune size and type varies coherently with lateral bars in the study reach (Figure 1-13). On the bar top, the A to A' topographic profile shows low resolution bedforms, discontinuous dunes with gaps in the trough and 2Dc dunes from the upstream to downstream end respectively (Figure 1-13). The B to B' bar slope profile shows 2Dc and dunes with gaps in the trough (Figure 1-13). On the B to B' profile the dune heights (H) are slightly larger than on the bar top and the position of the dunes with gaps in the trough is further downstream. Additionally, on the A to A' and B to B' profiles dunes with gaps in the trough are found before the profile reaches its crest. The C to C' bar slope

profile is mainly composed of 2Dc which increase in size at the downstream end as the bed elevation decreases (Figure 1-13). In the thalweg the D to D' profile shows 2Dc which decrease in size as the bed elevation decreases (Figure 1-13).

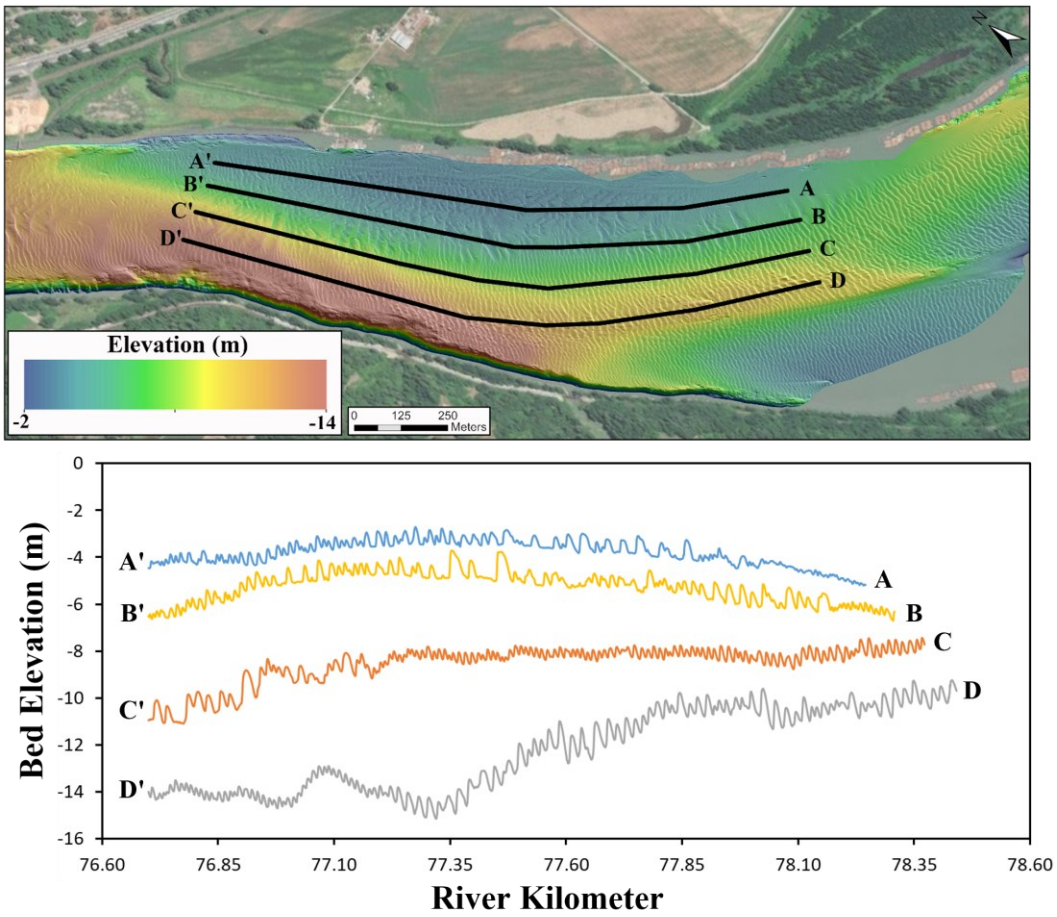

Figure 1-13. Topographic profiles through secondary meander bend III. A to A': bar top; B to B': upper bar slope; C to C': lower bar slope; D to D': Thalweg.

1.3.5. Spatial controls on dune dimensions

I examined relations between channel geometries (curvature, h_{ex}, S_t) and dune scaling relations (H/h, L/h). There is a strong correlation between curvature and depth excess (h_{ex}) with an r-square value of 0.78 (p-value = 6.19×10^{-7}) and a moderate correlation between curvature and transverse bed slope (S_t) with an r-square value of 0.55 (p-value = 4.28×10^{-4}). The correlation between metrics of channel geometry and dune characteristics is weaker. From a qualitative perspective, patterns of local maxima and local minima are generally consistent between channel geometry and dune

characteristics, but a lag exists (Figure 1-14). In the downstream direction, the channel geometries were generally observed to reach a local maxima before the dune scaling relations (Figure 1-14). Curvature has a modest statistically significant correlation with L/h (Figure 1-14c) and H/h (Figure 1-14f) with r-square values of 0.264 and 0.334, respectively. Similarly, depth excess has a modest statistically significant correlation with L/h (Figure 1-14b) and H/h (Figure 1-14e) with r-square values of 0.246 and 0.333 respectively. Transverse bed slope is not correlated with L/h (Figure 1-14a) or H/h (Figure 1-14d).

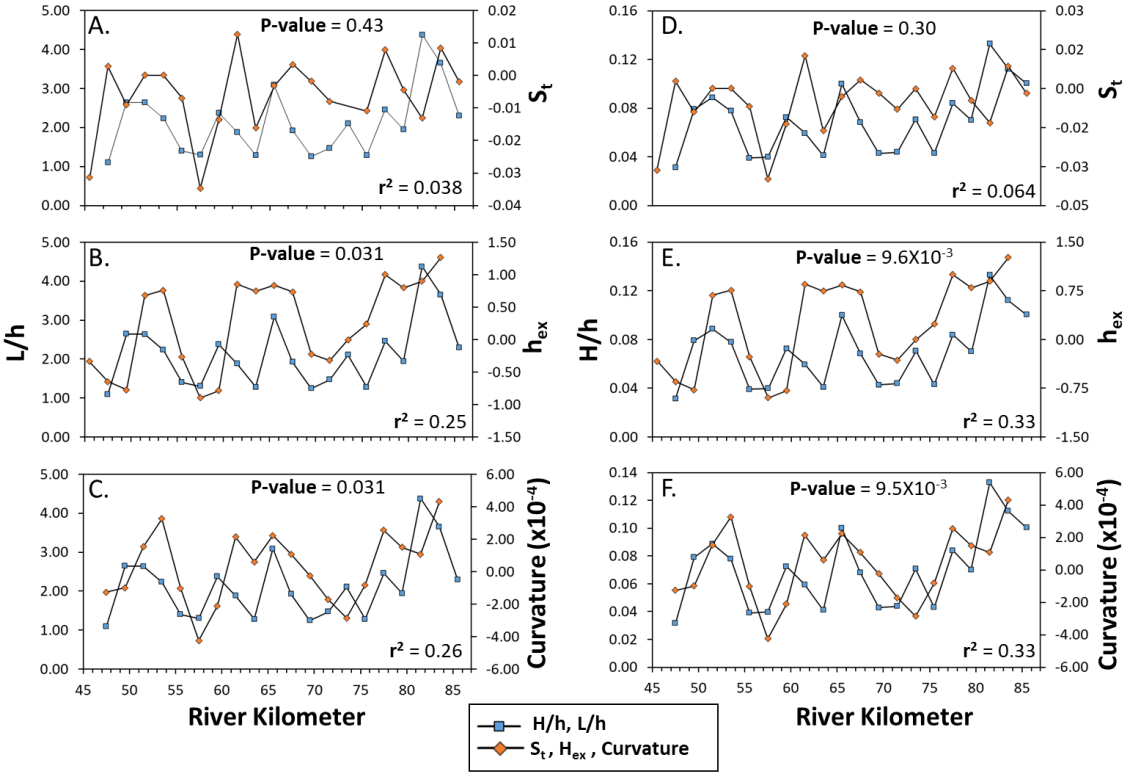

Figure 1-14. Downstream change in (A) channel curvature; (B) depth excess (h_{ex}); (C) transverse bed slope (S_t) for bedform length normalized by depth (L/h) and (D) channel curvature; (E) h_{ex}; (F) S_t for bedform height normalized by depth (H/h). The data was smoothed using a 2-km moving average.

1.4. Discussion

1.4.1. Do the bedforms observed in the lower Fraser River follow expected patterns?

In alluvial sand-bedded rivers it is often implied that dunes are ubiquitous and spatially uniform. My results show that bedforms are not ubiquitous or spatially uniform in natural channels, where ~20% of the entire bed surface area in the study reach was classified as non-bedforms (Fb/NbD). I also show that there is a wide range of dune scaling relations (H/L, H/h, L/h) within a river reach and that there does not appear to be a dominant or characteristic dune size. Dune scaling relations assume dune H scales as 1/6h and L as 5h (Yalin, 1964). My results show that dune size does not increase with h, supporting observations in Bradley & Venditti (2017), but our results also show that the variation within a river reach is so large that it is unreasonable to expect a single scaling relation to emerge for a reach. Therefore, assuming bedforms are ubiquitous and spatially uniform is an inaccurate representation of riverbed surfaces in natural sand-bedded channels and must be considered in flow resistance equations used to model river systems and paleo-flow reconstructions.

Observations of the spatial distribution of bedform types in natural meandering channels are limited. Previous observations of bedforms in river channels suggest that the largest dunes are found in mid-channel positions in meandering channels (Stein, 1965; Jackson, 1975) particularly on the shallower, inside edge of a meander bend (Wu et al., 2021). In the study reach the largest dunes were found on the bar slope downstream of secondary meander bend apices which is consistent with previous observations. The presence of the largest dunes on the inside edge of meander bends suggests that this is a location in a meandering channel where substantial sediment deposition occurs allowing for the formation of large dunes.

Highlighting the spatial variability of bedforms, bed configuration observations suggest that the dominant bedform type on point bar surfaces are dunes with curved crestlines (2Dc in our classification) (Bridge, 2003), while straight crested dunes (2Ds), ripples and upper-stage plane beds are also typically found on bar tops (Levey, 1978; Bridge, 2003). The edges of channels have been recognized to be composed of lower stage plane beds/ripples (Jackson, 1975; Allen, 1982). Others have found straight

crested dunes (2Ds) and straight to sinuous crested dunes (2Dc) in the straight sections of the channel between bends (Levey, 1978). My results are generally in agreement with field observations of bedforms on bar tops where continuous 2Dc dunes were the most abundant (~43% of bar top surface area) with flatbed and unclassifiable bedforms existing too. Straight sections were composed of continuous 2Dc and 2Ds dunes which agrees with field observations. However, no previous study has noted the presence of discontinuous dunes on bar tops, and specifically focused on the downstream end of lateral bars on the bar slope.

1.4.2. Are the patterns and distribution of bedforms observed linked to coherent variation in the channel?

In the study reach, a series of lateral bars align with secondary meander bend apices in the main channel. On these bar features a consistent sequence of bedforms was observed where Fb/Lr bedforms, discontinuous GiT dunes, and continuous 2Dc dunes were observed in the downstream direction. Similarly, sequences of bedforms were observed in straight sections of the channel in between two meander bends where Fb/Lr bedforms were observed in the thalweg with 2Ds and 2Dc dunes adjacent ascending in elevation out of the thalweg. Consistent bedform patterns in straight and meander bend segments of the river highlights that the pattern of bedforms observed is likely linked to the coherent variation in channel morphology which is influenced by channel currents. Observations of bedforms in meandering rivers are generally limited to localized reaches and consistent sequences of bedforms have not been previously observed through an entire reach of a river.

There are relations between bedform patterns and variation in the channel. Higher values of dune L/h and H/h scaling relations were aligned with secondary meander bend apices throughout the study reach which implies there may be a dynamic related to channel geometry which impacts the morphology of the dunes present. Supporting this idea, a modest statistically significant relation was found between channel geometries (curvature, h_{ex}) and dune dimensions (L/h, H/h). However, further work is required to confirm the influence of flow dynamics on sediment deposition and bedform sequences.

1.4.3. Why are there low sand supply dunes in a sand bed river?

On bar tops a common sequence of bedforms was observed in the downstream direction with Fb/Lr bedforms, discontinuous dunes (Brchn; GiT) and 2Dc dunes progressing from the upstream to the downstream end which is consistent with increasing sand supply to the bed in a low sand supply condition (Kleinhans et al., 2002; Venditti et al., 2019). The presence of bedforms associated with a low sand supply condition may be related to upstream staging of sediment. Substantial quantities of sand accumulates downstream of the GST (~RK 100.5) during low to moderate freshet conditions (Attard et al., 2014), while in higher freshet conditions (>10,000 m^3 sec^{-1}), it is suggested that sand accumulation from low freshet conditions is transported and re-distributed downstream (Venditti et al., 2019). It is possible that sand is staged upstream of the study area, downstream of the GST, and a freshet with high flow conditions is required to mobilize and redistribute sand further downstream replenishing the study area. Another consideration is that there is a reduction in sediment supply to lower Fraser River (Haught & Venditti, 2023) reducing the availability of bed material sediment to replenish the lower Fraser River. However, the consistent nature of a bedform sequence representative of increasing sediment supply on bar tops throughout the 35-km study reach suggests that this supply limitation is localized to this specific channel feature. The reason supply-limited bedforms are localized to this channel feature may be the result of sand accumulation in the thalweg of the channel which is not actively transported on bar tops during low flow conditions. The reason low sand supply dunes are present in the study reach is unclear but requires further examination.

Bed material sampling on a bar slope, where discontinuous dunes were observed on the 2021 low flow bathymetry, revealed the presence of bimodal sand and gravel. The bed material samples were not collected at the same time as the bed elevation data, but given the flows remained below 5,000 m^3 sec^{-1}, the threshold for significant sediment transport (McLean et al., 1999; Attard et al., 2014), I can predict that the bed surface was representative of a discontinuous dune field as depicted on the bathymetry map. The presence of these discontinuous dune fields with a sand gravel mixture on bar top surfaces may be the result of a local condition related to sediment transport of gravel and sand mixtures where superior mobility of gravel over sand enhances gravel transport rates in river channels (Venditti & Church, 2014).

1.5. Conclusions

Bedform distribution, dune scaling relations, channel characteristics and bed material grain-size throughout a ~35-RK reach of the sand bedded portion of the lower Fraser River were examined. Full channel bed topography surveys collected during winter low flow conditions with a MBES provided an exceptional opportunity to examine bedform spatial variability in a large sand bedded river. The results show that:

1. Bedforms are not ubiquitous in sand-bedded rivers and substantial bedform spatial variability was observed.
2. The patterns of bedforms observed are generally in agreement with previous field investigations and lateral accretion/point bar models used to interpret sedimentary deposits.
3. The variation in dune scaling relations (H/L, H/h, L/h) in the downstream direction is linked to bed geometry, specifically curvature and depth excess.
4. The presence of discontinuous dunes on bar tops is associated with patches of gravel and indicates that sand supply to the bar tops is currently limited.

The results suggest that bedforms are not ubiquitous in sand bedded rivers and that substantial bedform spatial variability exists. What ultimately controls the coherent variation of bedform types is unclear. However, bed geometry (e.g., curvature, depth excess), sand supply, and bed material grain-size appear to be important considerations. Future work should investigate the implications of bedform spatial variability in flow resistance and paleo-flow equations.

Chapter 2. Sediment Delivery to the Fraser Delta, British Columbia

Abstract

Anthropogenic development (e.g., sediment dredging, river training structures, dikes) has altered sediment dynamics of many large lowland rivers and their accompanying deltas. Development has been linked to systematic bed degradation and reduced sediment loads to delta fronts impacting the natural sediment budget of these large lowland rivers, creating management challenges. The sediment budget of the lower Fraser River in Southwest British Columbia has previously been estimated for the periods from 1963 to 1974 and 1974 to 1984 to estimate sediment delivery to the Fraser Delta. Examination of the sediment budget components using more recent information suggest substantial changes in riverbed topography and secular changes in sediment delivery. Here, I compile and analyze historic and contemporary sediment flux, bed topography, and riverbed dredging records to estimate the bed material sediment budget of the lower Fraser River and sediment delivery to the Fraser Delta. I find that i) historic sediment flux data at Mission overpredicts the current annual total sediment load delivery by ~43%; ii) substantial bed degradation occurred from New Westminster to Mission between 1991 to 2004, following extensive dredging of the navigational channel in the delta channels from 1975 to 1991; iii) bed material sediment extractions in the delta channels exceed the average annual sediment delivery to the Fraser Delta. The results indicate a bed material sediment deficit in the Fraser Delta that could destabilize the delta channels. I also propose several different sediment budget scenarios to provide insight on how the sediment budget may be altered as a result of different sediment extraction and delivery scenarios. Without monitoring and oversight of the lower Fraser River's sediment budget, anthropogenic impacts on the delta (e.g., bed level lowering, delta channel degradation) will become more apparent.

2.1. Introduction

Sediment dynamics are regularly disrupted in large alluvial rivers as a result of anthropogenic development (e.g., dredging, river training structures, dams). These human impacts have been linked to systematic channel degradation and diminished

sediment yields to delta fronts that may impact a system's natural sediment budget, creating management challenges related to channel stability, flooding, and coastal erosion (e.g., Wasson, 2003; Syvitski et al., 2005; Wang et al., 2007; Allison et al., 2012; Nelson et al., 2017; Kondolf et al., 2018; Nienhuis et al., 2020; Zhou et al., 2020). Over the past 60 years, sediment delivery to the world's deltas has declined by ~50% (Syvitski, Anthony, et al., 2022), which has resulted in a transition from a delta growth to a delta shrinking phase throughout the Anthropocene (Syvitski, Angel, et al., 2022).

A sediment budget is a framework developed to understand the distribution of sediments in a river reach for a specific period of time. Budget analyses often highlight sedimentation concerns (e.g., riverbed aggradation/degradation, reduced/increased sediment loads). Sediment budgets calculate the topographic change in a river reach as the change in sediment storage:

$$\Delta \mathrm{V}_{\mathrm{chan}} = \mathrm{V}_{\mathrm{in}} - \mathrm{V}_{\mathrm{out}} \qquad \text{Equation 2-1}$$

where V_{in} is the volume of sediment input (supply), and V_{out} is the volume of sediment output. Additional variables, such as the net mass of sediment removed from the channel by humans (V_{dredge}) and the net mass of dredged material disposed within a reach (V_{spoil}) may also require consideration. To account for the additional variables, Equation (2-1) can be re-written as follows:

$$\Delta \mathrm{V}_{chan} = \mathrm{V}_{in} - \mathrm{V}_{out} - \mathrm{V}_{dredge} + \mathrm{V}_{spoil} \qquad \text{Equation 2-2}$$

Here, I examine the sediment budget of the lower Fraser River in southwest British Columbia. In this study the lower Fraser River refers to the reach of the river from Mission (RK 85) to Sand Heads (RK 0). I estimate the 'natural' and 'modern' sediment budgets using estimated sediment delivery to the Fraser Delta based on previous investigations. The 'natural' sediment budget balances sediment inputs, outputs and change in storage prior to anthropogenic alterations, while the 'modern' budget accounts for anthropogenic alterations to sediment storage. Then I calculate the 'contemporary' sediment budget using new observations of sediment flux, as well as historical and recent surveys of the river. The contemporary results are compared to the natural and modern estimates of sediment delivery to the Fraser Delta.

2.1.1. Study Site

The Fraser River drains ~232,000 km^2 of British Columbia, Canada. Emerging from a 375 km long bedrock canyon near Hope, British Columbia (RK 165; where RK is river kilometers upstream of the river mouth at Sand Heads), the Fraser River deposits its gravel load between RK 185 and ~RK 100.5 (Figure 2-1a). At Yaalstrick Bar (RK 100.5), a change in river gradient and washload deposition causes a gravel-sand transition (GST) ~15 km upstream of Mission (RK 85) (Venditti & Church, 2014) (Figure 2-1a). Downstream of Mission (RK 85), the lower Fraser River is a single thread, sand-bed channel with bends that have back channels in the apices. The channels are not actively meandering because most of the flow is carried through the inside of bends rather than the apices (Venditti & Church, 2014). Engineering controls (e.g., riprap, dikes, jetties etc.) have also contributed to fixing the current position of the lower Fraser River. In the sand bed reach, sand is carried as suspended bed material load and bedload in the form of migrating dunes (Kostaschuk et al., 1989; Ilersich, 1992; Hendershot et al., 2016; Venditti et al., 2019). The bed material-wash load division is 0.177 mm (McLean et al., 1999; Attard et al., 2014), and the sand bed has a median size of ~0.385 mm with no downstream fining through the sand reach (Venditti & Church, 2014) (Figure 2-1b).

Fraser River discharge is snowmelt dominated with a prolonged freshet period of high flow, generally peaking from late May to early July before receding in August and September. The mean annual flow at Mission (Water Survey of Canada gauging station 08MH024) from 1983 to 2013, was 3,183 $m^3 s^{-1}$, and the mean annual flood was 9,534 $m^3 s^{-1}$ (Haught et al., 2017). The flood of record at Mission, in 1894, was estimated to have peaked at a flow of 17,200 $m^3 s^{-1}$ (McLean et al., 1999). A tidal influence is present downstream of the GST; at Mission, the tidal influence ranges from a few a centimeters during high flow freshet periods to ~1 m during winter tides (Attard et al., 2014). The river bifurcates at New Westminster (RK 35), forming the Fraser Delta (Figure 2-1a).

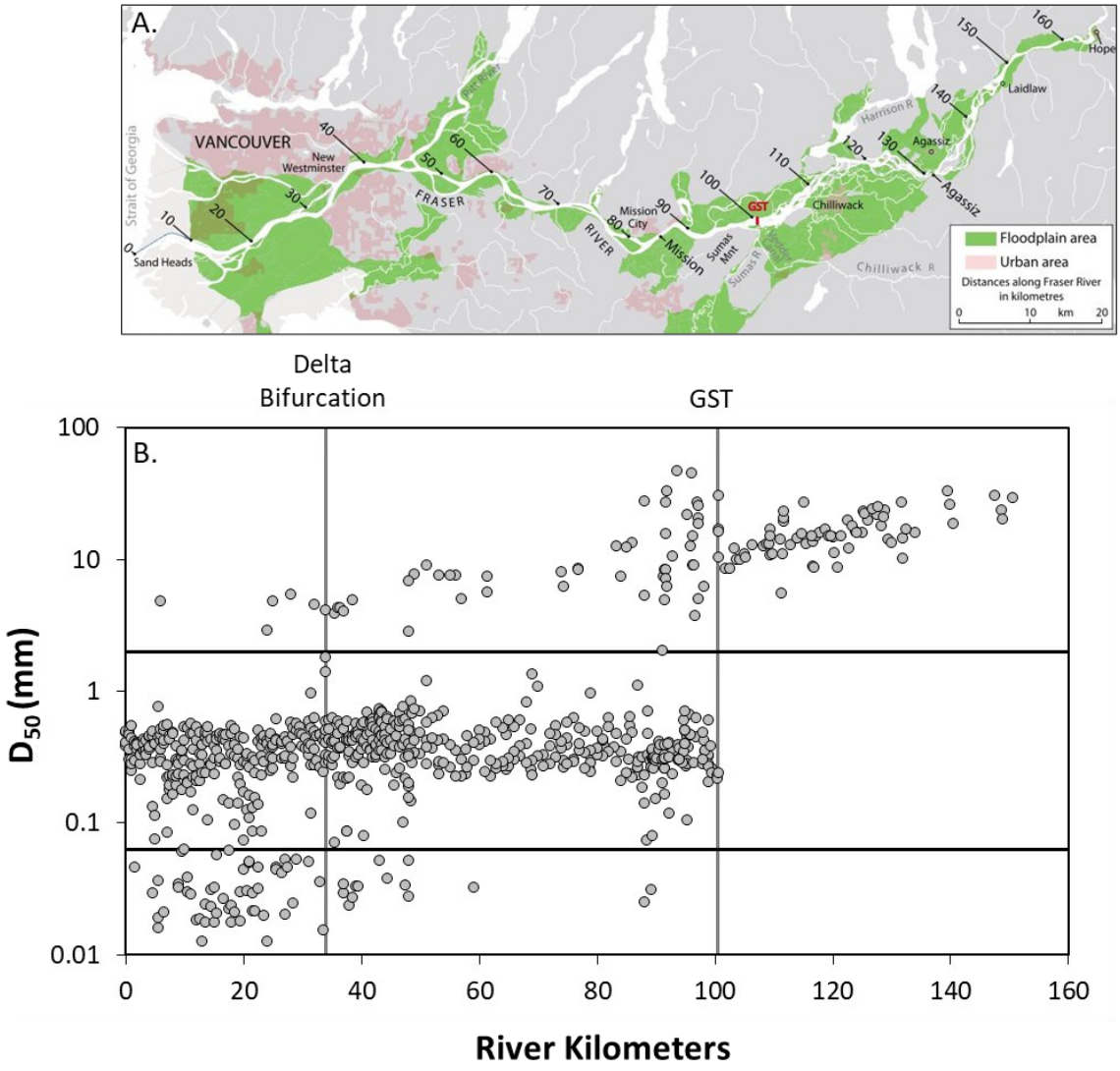

Figure 2-1. (A) The Fraser River downstream of Hope, British Columbia. Modified from Venditti & Church (2014). (B) Downstream change in median grain-size (D_{50}). The grain-size data used to generate this figure are derived from the following sources: McLaren & Ren, 1995; Venditti & Church, 2014; McLean, 1990; Ham, 2005. The thick black lines represent the delineation between silt/clay and sand, and sand and gravel.

2.1.2. Previous Sediment Budget Estimates

A sediment budget for the lower Fraser River from Mission (RK 85) to Sand Heads (RK 0: the mouth of the Fraser River) was estimated for the periods between 1964 to 1973 and 1974 to 1984 based on i) bed material sediment flux at Mission, ii) published dredging records, and iii) observed bathymetric changes using historical

surveys of the Fraser downstream of Mission (McLean & Tassone, 1991). Sediment output to the Strait of Georgia was estimated by rearranging and restating Equation (2) as follows:

$$V_{out} = V_{in} - \Delta V_{chan} - V_{dredge} \quad \text{Equation 2-3}$$

The sediment budget was re-examined for the interval between 1998 to 2001 based on: i) sediment flux estimates for 1966 to 1986 (McLean et al., 1999), ii) published dredging records (1961-2001), and iii) topographic bed level changes between 1963 to 2001 downstream of New Westminster and 1951 to 1998 from RK 45 (upstream of New Westminster) to RK 76 (near Crescent Island) (Northwest Hydraulic Consultants, 2002). Previous budget estimations were mainly focused on the reach of the lower Fraser River from Port Mann (RK 42) to Sand Heads (RK 0). Other than some localized cross-section comparisons of bed elevations, the previous budgets did not extend upstream to Mission, where sediment transport measurements have been taken to establish the bed material load of the Fraser River. More recent examinations of bed topography and water level changes in the lower Fraser have shown bed degradation (e.g., McLean et al., 2006; Nelson et al., 2017), but are typically limited to local areas in the river.

Previous estimates of the sediment budget components for the lower Fraser (e.g., McLean & Tassone, 1991; McLean et al., 1999, 2006; NHC, 2002) can be used to establish the natural and anthropogenically-impacted sediment budget of the Fraser Delta. Observations of sediment flux at Mission from 1966 to 1986 indicate that the historic sediment flux at Mission was 17 Mt yr^{-1}, of which 2.7 Mt yr^{-1} was clay, 8.3 Mt yr^{-1} was silt, and 6.1 Mt yr^{-1} was sand (McLean et al., 1999). The vast majority of this sediment is carried as washload (< 0.177 mm) during the freshet without forming widespread, persistent deposits on the channel bed or banks. Approximately 3.2 Mt yr^{-1} of the sand component (> 0.177 mm) is carried as bed material load which is sediment sourced from the channel bed and lower banks of rivers and is chiefly responsible for building channel morphology (McLean et al., 1999). The bed material load consists of 3.0 Mt yr^{-1} of sand carried in suspension and 0.15 Mt yr^{-1} is moved as bedload, accounting for 19% of the total sediment flux (McLean et al., 1999). The natural sediment budget can be estimated by assuming the channel was in a state of equilibrium where there was no historical change in bed elevation between Mission (RK 85) and New Westminster (RK 35). In the delta channels, we assume ~5% of the sediment

supplied to the reach was deposited (~0.2 Mt yr^{-1}) as the main channel approaches the mouth of the river at Sand Heads (RK 0) (Figure 2-2). Channel migration documented by Clague et al., (1986) suggests that backwater induced deposition that likely extended upstream into the delta channels. Under these assumptions, ~3.0 Mt yr^{-1} of bed material would have been delivered to the delta front before anthropogenic impacts on the river (Figure 2-2). This bed material built the modern delta and tidal flats that surround the delta through channel migration and avulsion (Mathews & Shepard, 1962; Clague et al., 1983).

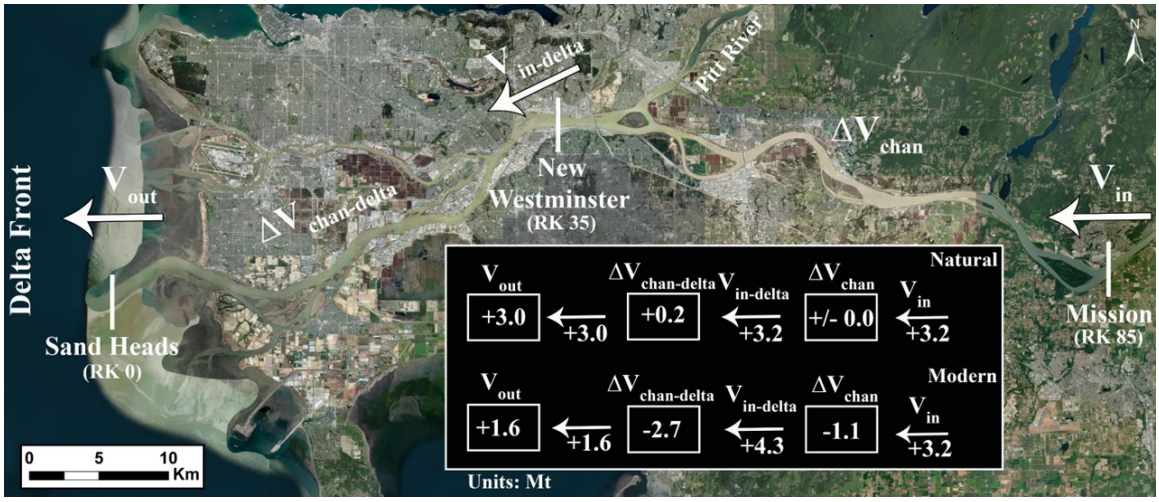

Figure 2-2. The estimated natural (prior to anthropogenic interference) and modern (anthropogenically-impacted) sediment budget for the lower Fraser River, British Columbia (McLean et al., 1999, 2006; Northwest Hydraulic Consultants, 2002).

The anthropogenically-impacted sediment budget can be estimated assuming that the natural sediment influx of bed material to Mission is ~3.2 Mt yr^{-1} (V_{in}), incorporating the effects of dredging (V_{dredge}), and any changes in bed elevation (ΔV_{chan}) (Figure 2-2). McLean et al. (2006) suggested that decline in water level gauge datums at New Westminster between ~1970 and 2000 are related to systematic bed lowering and dredging on the lower Fraser River. Additionally, survey comparisons from 1952 to 2005 show ~34 Mt of bed degradation which is equivalent to 1.6 Mt yr^{-1} (McLean et al., 2006). It has been hypothesized that this lowering is a result of upstream migration of a knickpoint resulting from dredging in the delta channels (McLean et al., 2006). Assuming the majority of bed degradation observed by McLean et al. (2006) occurred after 1974 when dredging intensity increased in the delta channels, then a storage change of -1.1 Mt yr^{-1} occurred in the reach between Mission and Port Mann between

1974 and 2005 (Figure 2-2). Therefore, ~4.3 Mt yr^{-1} of bed material was delivered to the delta after the dredging program began (Figure 2-2). Of that sediment delivered, ~2.7 Mt yr^{-1} was dredged from the main channel between 1961 and 2005 (not including a period of intense dredging that occurred from 1974 to 1994) to maintain deep-water shipping ports in the Fraser Delta (Figure 2-2). Under these assumptions, the modern bed material sediment output to the delta front would be ~1.6 Mt yr^{-1}, which is ~1.4 Mt yr^{-1} less than what was delivered historically (Figure 2-2).

Since the initial examinations of the lower Fraser River sediment budget (McLean & Tassone, 1991; McLean et al., 1999), there has not been a systematic analysis of the sediment budget that incorporates new observations of sediment inputs and changes in bed elevation. Observations of V_{in} in the historical and modern sediment budget estimates reported above are based on sediment flux measurements at Mission measured by the Water Survey Canada (WSC) between 1966 and 1986, but that record extends to 1992 only. More recently, measurements of the sediment load at Mission have been made between 2010 and 2014 using conventional methods and hydro-acoustics (Attard et al., 2014; Venditti et al., 2016; Haught, 2017; Haught et al., 2017, 2020; Haught & Venditti, 2023). The 2010 flux measurements at Mission yielded an exceptionally small sediment load during one of the lowest freshet flows on record but the measured values are consistent with the trend of historical records (Attard et al., 2014). Sediment load measurements collected from 2012 to 2014 at Mission are systematically lower than historical WSC observations, which may indicate a shift in sediment supply to the system that requires further investigation (Haught et al., 2017, 2020; Haught & Venditti, 2023). A comparison of contemporary (2010, 2012-2014) and historical (1966-1991) sediment flux measurements is required to estimate the contemporary sediment supply to the lower Fraser River and delta.

Change in sediment storage (ΔV_{chan}) has been difficult to incorporate into Fraser River sediment budgets because past surveys had low spatial and temporal resolution (e.g., McLean et al., 2006; Northwest Hydraulic Consultants, 2002). However, there are high spatial resolution surveys in 1951/1952, 1991, and a series of surveys from 2000 to present. Public Service and Procurement Canada (PSPC) now routinely surveys the lower Fraser River collecting high-resolution bathymetric data which produces detailed bed level information that can be used to quantify ΔV_{chan}.

2.1.3. Mission Statement

The goal of this study is to compare the natural, modern, and contemporary sediment budgets for the lower Fraser River and estimate sediment delivery to the Fraser Delta. I present bed topography changes in the Main Arm of the lower Fraser River from RK 47 to 85 by comparing a series of bathymetric surveys between 1951 to 2021. I also compiled i) reported sediment dredging (1961-2013), ii) sediment disposals at sea (2010-2020), which allows me to estimate dredging volumes from 2014 to 2020; iii) historical (1966-1992) and contemporary (2010, 2012-2014) sediment flux data. The specific questions I address are: i) How have bed levels changed through time in the reach from Mission to New Westminster (upstream of the Pitt River confluence); ii) What is the current sediment delivery to the Fraser Delta based on the sediment budget; iii) How has sediment delivery to the delta front changed due to anthropogenic sediment removals; iv) What are the projected changes in sediment delivery based on different V_{in} and V_{dredge} scenarios? I end with considerations of the long-term impacts of a reduced sediment supply to the delta and the work necessary to better constrain sediment budget components of the lower Fraser River and Delta.

2.2. Methods

2.2.1. Sediment Delivery (V_{in})

Historical and contemporary sediment flux data from Mission (RK 85) was compiled to assess a potential change in sediment delivery (V_{in}) to the lower Fraser River. The historic data was collected by the Sediment Survey Section of the Water Survey of Canada (WSC) sediment transport program, which operated from 1966 to 1992. Observations consist of daily river discharge (Q_{daily}) and suspended sediment concentrations at Mission. Concentration measurements are from both point-integrated and depth-integrated samples collected using P61 or P63 sediment samplers. Point-integrated sediment samples were collected in a cross-section of five evenly spaced vertical profiles, each with 4 to 7 measurement points, that are depth-averaged and then width-averaged to derive channel-averaged concentration. The channel-averaged concentration is then multiplied by Q_{daily} to get the daily total suspended sediment flux (Q_{ss-tot}). Point integrated sampling was undertaken periodically during the annual high

flow season. Depth-integrated sediment flux concentrations are measured in one vertical profile in the channel center over a wider range of discharges and daily during the high flow season. The point-integrated samples are considered the true sediment flux because they capture the cross-stream variation in sediment concentration, while the depth-integrated data only measures the centerline concentration. Therefore, the depth-integrated data needs to be corrected to represent the true sediment flux (McLean et al., 1999). To correct the depth-integrated data, WSC developed an empirical relation between depth-integrated and point-integrated concentrations collected at the same time (McLean et al., 1999). Then, the depth-integrated correction is applied to published sediment concentrations at Mission (gauging station 08MH024) by the WSC.

The contemporary flux data consists of point-integrated measurements obtained during the 2010 and 2012 to 2014 hydrographs (Attard et al., 2014; Haught, 2017; Haught et al., 2020; Haught & Venditti, 2023). Point-integrated measurements were collected in a cross-section of five evenly spaced vertical profiles, each with 5 to 6 measurement points. For both historical and contemporary data sets, Q_{ss-tot} is separated based on grain size to obtain the suspended bed material flux (Q_{ss-BM}) for > 0.177 mm sand.

Regression relations were derived from the historical and contemporary sediment flux data and Q_{daily} at Mission to compare the annual sediment load of bed material (Q_{BM}) delivered to the delta channels. For the historical data, I used the regression equation derived in McLean et al. (1999) between Q_{ss-BM} and Q_{daily} which used WSC data from 1966 to 1986. The McLean et al. (1999) regression is between depth-integrated samples corrected using the WSC correction and point-integrated profiles that were collected at flows > 5,000 m^3 sec^{-1}. For the contemporary data, new regression equations were derived using flux data from 2010 to 2014. The regression relations were then used to predict the daily Q_{ss-BM} for the historical (1966-1992) and contemporary (2010-2014) periods, which were summed to estimate the annual Q_{ss-BM}. Bedload comprised a small but not negligible component of the total bed material flux.

McLean et al. (1999) provides a regression relation between daily bedload flux and Q_{daily} at Mission based on measurements from 1966 to 1986 that shows bedload flux is ~5% of annual Q_{ss-BM}. Therefore, total bed material load was calculated as

$$Q_{BM} = 1.05 \sum Q_{ss-BM}$$ Equation 2-4

Discharge is generally published by WSC at Mission when Q_{daily} > 5,000 m^3 sec^{-1} based on the rating curve established for the gauging site because of the tidal influence on water levels. The fluvial component of discharge at Mission was estimated as the sum of Q_{daily} at the Hope (8MF005), Vedder River (8MH001), and Harrison River (8MG013) WSC gauging stations when Q_{daily} < 5,000 m^3 sec^{-1} for the previous day to account for the time lag between the gauging sites.

2.2.2. Change in Sediment Storage (ΔV_{chan})

Bed elevation data is derived from bathymetric surveys of the Main Arm of the Fraser River from RK 85 (Mission, British Columbia) to RK 47 (the downstream end of Barnston Island, upstream of the Pitt River confluence) (Figure 2-3) collected in 1951/1952, 1991, 2003/2004, 2010, 2016, 2019, 2020/2021. The 1951/1952 surveys were collected by Public Works Canada (PWC) and the 1991 survey was collected by the Canadian Hydrographic Survey (CHS) using single beam. The point density of the historic surveys is variable. The 1991 CHS survey had a point spacing of ~50 m, while the PWC 1951/1952 survey had a cross-sectional point spacing of ~10 to 50 m, but the cross-sections were spaced ~100 to 200 m apart.

Bathymetric surveys completed from 2000 to 2021 were conducted by the Public Service and Procurement Canada (PSPC). PSPC has used a variety of instruments to collect positioning and bed elevation data. For example, the 2020/2021 survey used a Kongsberg 2040C Dual with a Real Time Kinematic GNSS to collect the bed topography data. An Applanix POS MV inertial guidance system was used to measure vessel heading, pitch, heave and roll. Raw bed elevation data were processed to correct for tidal stage, pitch, heave, roll and sound velocity, and to remove spurious data points. PSPC generally collects single beam (SBES) and multi beam echosounder (MBES) data of the navigational channel on an annual schedule. Recently, MBES instrumentation has allowed PSPC to increase the spatial coverage of the surveys and has started surveying upstream of New Westminster (RK 35) to Mission (RK 85) more frequently. MBES data yields a point density of <0.5m resolution, while SB data yields a cross-sectional point density of ~1 m, but generally cross-sections are spaced ~100 m apart. The 2003/2004, 2010 and 2016 PSPC surveys are composed of SB data, the 2019 survey is composed

of SB (channel edges) and MB (navigational channel) data, and the 2020/2021 survey is composed of MBES data. All bathymetric data were referenced to the Canadian Geodetic Vertical Datum 1928 (CGVD28).

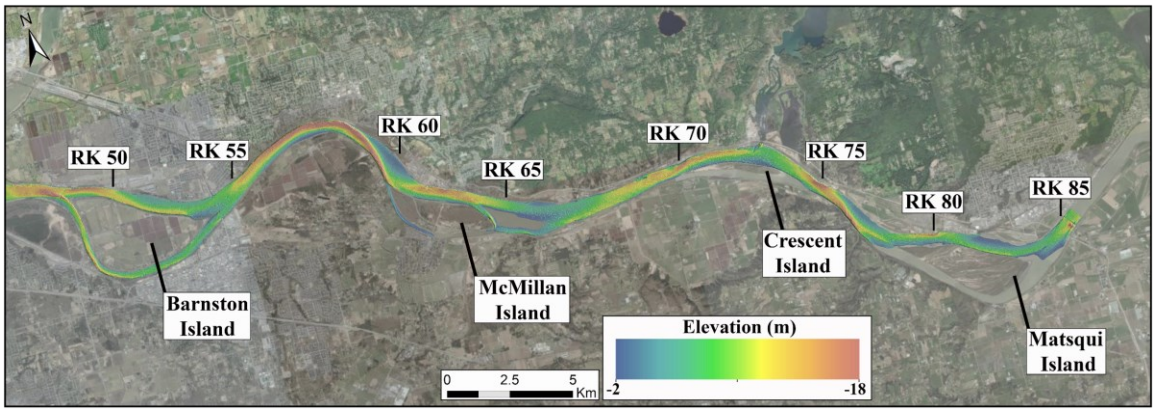

Figure 2-3. Multi-beam echosounder (MBES) bed topography of the lower Fraser River (RK 85-47). Bed elevation data was collected during 2020/2021 low flow conditions by the Public Service and Procurement Canada (PSPC). Bed elevations are relative to the Canadian Geodetic Vertical Datum 1928 (CGVD28).

All data were gridded at a 10x10 m resolution to create raster surfaces to compare bed topography. The raster surfaces between years were differenced to calculate the change in bed elevation (ΔV_{chan}), the sum of bed elevation changes between the two rasters. Saturation curves were generated to determine how different spatial resolutions impacted the change in bed elevation between raster surfaces. At spatial resolutions greater than 10x10 m, ΔV_{chan} becomes dependent on the horizontal resolution, but below 10x10 m the result is not, so I selected a spatial resolution of 10x10 m for all bathymetries. A centerline profile was also generated and bed elevations were extracted from the raster surfaces for the 1951/1952, 1991, 2003/2004, 2010, 2020/2021 survey years to further examine bed level elevation change through time.

2.2.3. Sediment Extractions (ΔV_{dredge})

Volumes of sediment extracted from the lower Fraser River through dredging (V_{dredge}) were compiled to assess the change in sediment storage in the delta channels ($\Delta V_{chan-delta}$) and delivery of sediment to the delta front (V_{out}). Sediment dredging in the lower Fraser River is generally concentrated in the delta channels, downstream of New Westminster (RK 35), to maintain draft depths associated with ocean-going vessels.

Dredging data from 1961 to 2013 for the South Arm of the Fraser River were extracted from records provided by the Port of Vancouver in published sources (Public Works Canada, 1957; McLean & Tassone, 1991; Northwest Hydraulic Consultants, 2002; British Columbia, 2017). This study only considers the South Arm of the lower Fraser River, dredging data from the North Arm was not considered. Prior to 1961 dredging records are generally unavailable or incomplete. However, from 1946 to 1956 it was reported that ~1.4x10^6 m^3 was removed from the Main Arm (Pretious, 1958). To my knowledge dredging records have not been released by the Port of Vancouver since 2013, but the volumes of sand disposed at sea by the Port of Vancouver dredging program have been reported to Environment and Climate Change Canada (ECCC) since 2010. ECCC records do not account for the volume of material transferred within the delta channels or sold, but they do provide some insight into the volume of sediment dredged from the channel and removed from the system. To extend the dredging time series from 2014 to 2020, I calculated the ratio (γ) of reported dredging volume (V_{dredge}) to the volume disposed at sea (V_{spoil}) for 2011 to 2013. I then apply this ratio to estimate V_{dredge} to V_{spoil} as:

$$\mathrm{V}_{dredge} = \gamma \times \mathrm{V}_{spoil} \qquad \text{Equation 2-5}$$

for the period 2014 to 2020.

2.3. Results

2.3.1. Sediment Supply (V_{in})

The total suspended sediment load (Q_{ss-tot}) is composed of wash load (Q_{ss-WL}; <0.177 mm) and suspended bed material (Q_{ss-BM}; >0.177 mm) sediment. Figure 2-4a-c shows the variation in measured sediment flux. Measured historic sediment fluxes come from point-integrated samples collected at discharges >5000 m^3 sec^{-1} and depth-integrated sediment samples collected between discharges of 600 to 13,600 m^3 sec^{-1} which are corrected to channel averaged values using the WSC method (Figure 2-4a-c). The minimum measured Q_{ss-tot} was 1.45x10^4 tonnes day^{-1} and maximum measured Q_{ss-tot} was 1.34x10^6 tonnes day^{-1} (Figure 2-4a). Measured Q_{ss-WL} varied between 1.41x10^4 and 7.52x10^5 tonnes day^{-1} (Figure 2-4b), while the range of measured Q_{ss-BM} varied between 1.55x10^2 and 7.11x10^5 tonnes day^{-1} (Figure 2-4c). Figure 2-4d-f shows

the contemporary sediment fluxes, which are from point-integrated samples collected over a wider range of discharges than the historical point-integrated measurements between discharges of 2,000 and 9,700 m^3 sec^{-1} (Figure 2-4d). Contemporary measured Q_{ss-tot} has a minimum of 2.70x10^3 tonnes day^{-1} and maximum of 2.67x10^5 tonnes day^{-1} (Figure 2-4d). The range of Q_{ss-WL} was from 2.58x10^3 to 1.83x10^5 tonnes day^{-1} (Figure 2-4e), while the range of Q_{ss-BM} was from 1.18x10^2 to 3.49x10^4 tonnes day^{-1} with an average flux of 9.51x10^3 tonnes day^{-1} (Figure 2-4f).

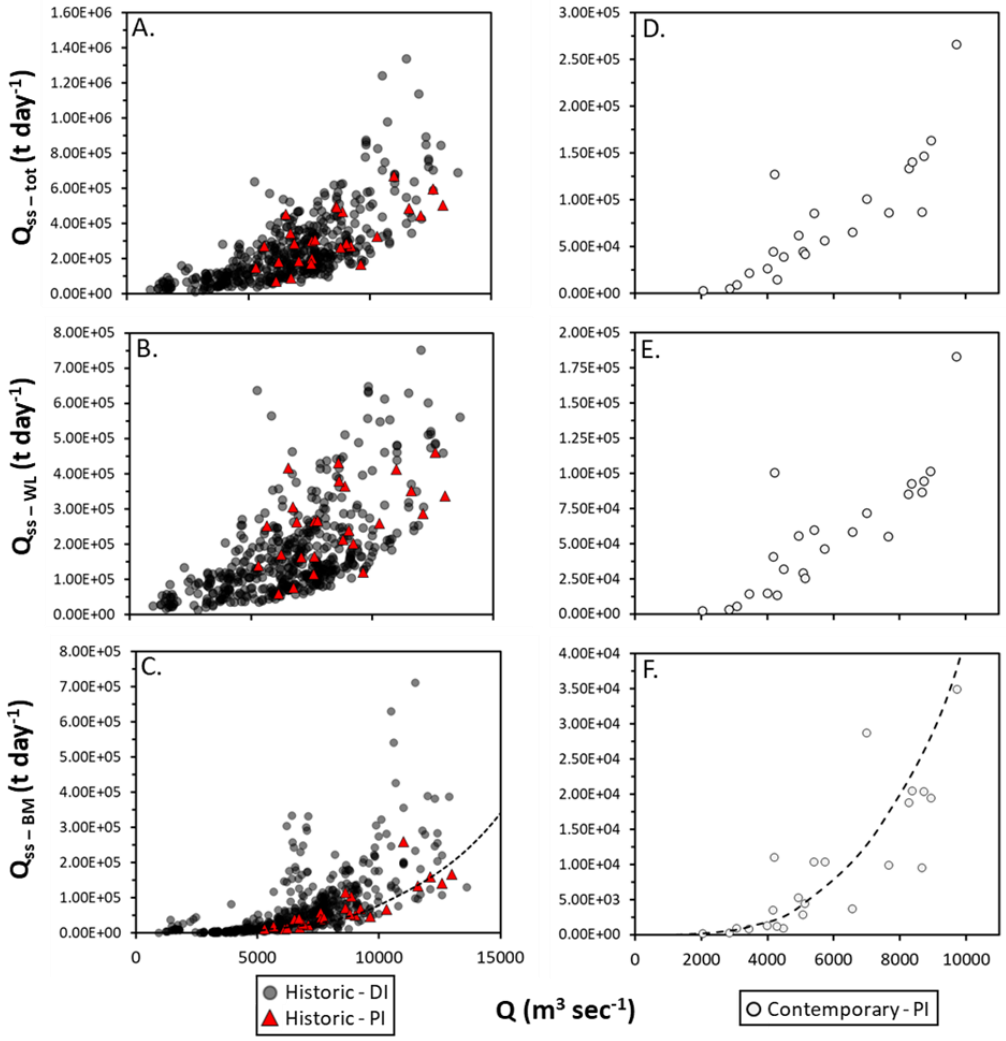

Figure 2-4. **Historical (1966-1991) point (PI; n=26) and depth-integrated (DI; n=458) suspended sediment flux samples (A-C) and contemporary (2010, 2012-2014) PI (n=23) suspended sediment flux samples (D-F). The suspended sediment flux samples are divided to show the separation of the total suspended sediment flux (Q_{ss-tot}) which is composed of washload (Q_{ss-WL}; < 0.177 mm) and bed material (Q_{ss-BM}; > 0.177 mm) fluxes. The dashed black lines in panel C and F are the regression relations, Equation (2-6) and Equation (2-7).**

McLean et al. (1999) used published WSC data (Figure 2-4a-c) to derive a relation between the measured channel-averaged concentration from the point-integrated and the depth-integrated samples to establish a correction factor for the depth-integrated samples. Then, using regression relations between daily Q_{ss-tot}, Q_{ss-BM}, and Q_{ss-WL} sediment fluxes and Q_{daily} a rating curve was established for Mission. I elected to use their rating curve to establish the historical suspended bed material concentration:

$$C_{ss-BM} = 3.73\ x\ 10^{-9}\ x\ {Q_{daily}}^{2.6} \qquad \text{Equation 2-6}$$

and calculate suspended bed material flux as

$$Q_{ss-bm} = C_{ss-BM} Q_{daily} = 0.0864\ x\ 3.73\ x\ 10^{-9}\ {Q_{daily}}^{(1+2.6)} \qquad \text{Equation 2-7}$$

where 0.0864 converts from mg l^{-1} to tonnes day^{-1}. The coefficient 3.73 x 10^{-9} differs slightly from Equation 3 in McLean et al. (1999) which is 3.46 x 10^{-9} but is consistent with the published annual fluxes at Mission which are reported (McLean et al., 1999). The reason for the difference is not obvious to me and I suspect it is a typographical error. Therefore, I elected to use the coefficient that gives the published annual fluxes and for which I have the original calculations.

Contemporary sediment flux is calculated from a regression relation between Q_{ss-BM} and Q_{daily}:

$$Q_{ss-bm} = BCF\ x\ 0.0864\ x\ 1.13\ x\ 10^{-8}\ {Q_{daily}}^{(1+2.38)} \qquad \text{Equation 2-8}$$

with an R^2 of 0.67 and is statistically significant at the 95% confidence interval (P-value < 0.05). A bias correction factor (BCF) derived following the methods of Duan (1983) was applied to the contemporary flux data to eliminate bias caused by log-transformation of the data to derive the regression relation.

For both the historical and contemporary estimates of Q_{ss-bm}, we follow McLean et al. (1999) and use Q_{daily} below > 5,000 $m^3\ sec^{-1}$ even though flows are tidally influenced. Therefore, we assume that the sediment supply movement is proportional to the fluvial discharge when averaged over the whole day because even though there may be times during that day when the actual discharge at the site is less than or greater than the daily value, instantaneous discharge must average to the daily value.

Fortunately, our calculations are not sensitive to this assumption because there is minimal sediment transport at discharges >5,000 $m^3 sec^{-1}$. Examination of the annual bed material flux (Q_{BM}) between the historical and contemporary periods reveals a clear reduction in Q_{BM} (Figure 2-5a). The historical mean annual Q_{BM} is 2.99 Mt yr^{-1} (1966 to 1991), but only 2.37 Mt yr^{-1} for the contemporary period (2010 to 2014). This observation suggests that there has been a reduction of ~0.62 Mt yr^{-1} in bed material delivered to the lower Fraser River at Mission from the historical to the contemporary period. I explored whether the reduction was a result of our calculation methods or derived directly from the point-integrated measurements. I compared the historical point-integrated measurements that were only taken at flows >5,000 $m^3 sec^{-1}$ with the point integrated contemporary measurements (Figure 2-5b). The fact contemporary measurements were taken at flows ranging from 2,000 and 9,700 $m^3 sec^{-1}$ and the historical measurements were taken only at flows > 5,000 $m^3 sec^{-1}$ gives the impression that they may be from one continuous relation, but closer examination reveals that where the measurements are taken at the similar discharges, the contemporary measurements are consistently less (Figure 2-5b).

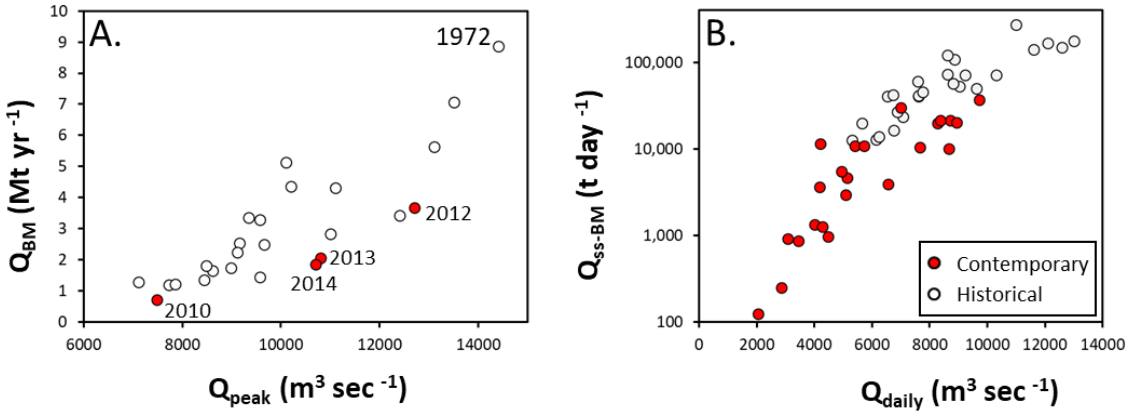

Figure 2-5. Annual bed material load (Q_{BM}) for the historical (1966-1991) and contemporary (2010, 2012-2014) measurement periods versus peak discharge (Q_{peak}) at Mission (A). Comparison of point-integrated Q_{ss-BM} collected during the historical and contemporary periods of sediment flux measurements versus Q_{daily} (B). Panel B only considers the historical point-integrated data. It does not consider the depth-integrated data which was used to derive the McLean et al. (1999) relation.

I projected the historical Q_{BM} forward using Equation 2-7 (Figure 2-6a) and found the predicted mean annual Q_{BM} is 2.65 Mt yr^{-1} for 1991 to 2009 and 3.54 Mt yr^{-1} for the

period between 2010 to 2020 but that assumes the historical rating curve applies at Mission after the historical measurement period (1966-1992). Using Equation 2-8 to calculate the contemporary Q_{BM} from 2010 to 2020, I find that the predicted mean Q_{BM} is 1.98 Mt yr^{-1} (Figure 2-6b). On average, from 2010 to 2020, the annual bed material flux using Equation 2-7 overpredicts Equation 2-8 by ~43% (Figure 2-6b).

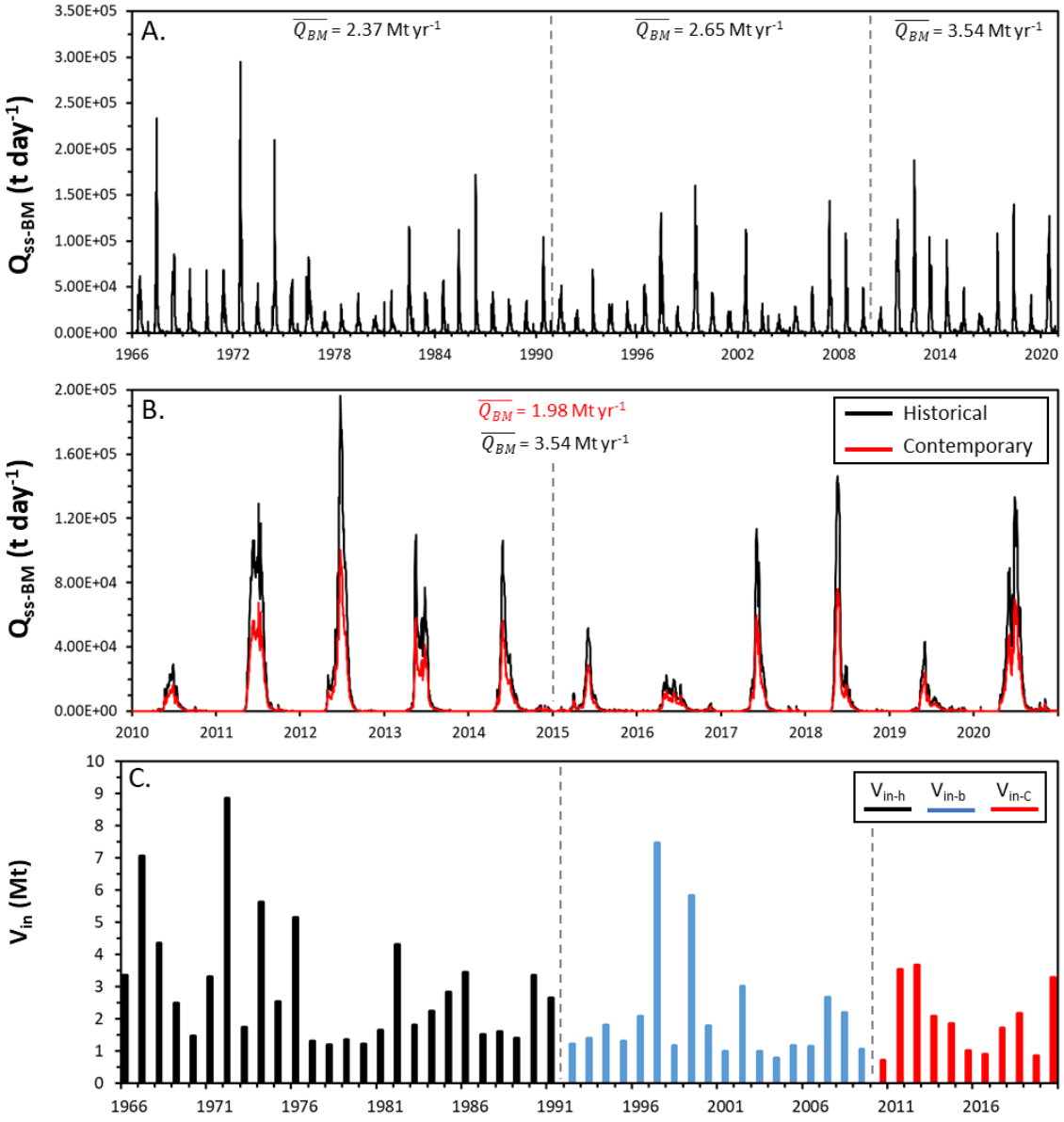

Figure 2-6. Suspended bed material ($Q_{ss\text{-}bm}$) sedigraph with projections to 2020 for the (A) historical (1966-1991) and (B) contemporary (2010-2014) periods. Comparisons of the historical and contemporary $Q_{ss\text{-}bm}$ show that the historical relation overpredicts the contemporary relation (B). The gray vertical dashed lines indicate the contemporary and historical sampling periods and the blended period (1992-2009). Sediment loads were estimated based on the regression relations (Equation 2-6, 2-7) derived from the historical and contemporary measurements of sediment flux at Mission. Time series of historical ($V_{in\text{-}h}$), blended ($V_{in\text{-}b}$) and contemporary ($V_{in\text{-}c}$) sediment supply from 1966 to 2020 (C).

In order to calculate V_{in}, I use the historical (1966-1991) annual bed material flux (Q_{BM-h}) from the integrated time series based on Equation 2-7 and the contemporary

(2010-2020) annual bed material flux (Q_{BM-c}) derived from Equation 2-8. For the interval from 1991 to 2010, I use a blended estimate of Q_{BM} calculated as

$$Q_{BM-b} = \frac{a}{19} Q_{BM-h} + \frac{19-a}{19} Q_{BM-c} \qquad \text{Equation 2-9}$$

where a is the number of years since 1991. In 1991 $V_{in-b} = V_{in-h}$ and in 2010 $V_{in-b} = V_{in-c}$, but between 1991 and 2010, V_{in-b} is a linear function between V_{in-h} and V_{in-c}. The blended approach produces an annual time series of the Q_{BM} volumes delivered to the delta which are derived from the sediment rating curves that overlap with the underlying data and that represent the gradual shift from Equation 2-7 to Equation 2-8 between 1991 and 2010. I assume that the contemporary rating curve is still accurate past the period of measurements. However, the applicability of the contemporary rating curve can only be confirmed with continued observations of sediment flux at Mission.

2.3.2. Changes in Bed Level (ΔV_{chan})

Over the past 70 years the Main Arm of the lower Fraser River from Mission to New Westminster has been dominated by degradation (Figure 2-7). In some locations the bed has degraded by up to 5 m (Figure 2-7). However, there are a few areas where aggradation has occurred, most notably at the Mission Rail Bridge, around the northern bank and downstream of Matsqui island, and north of McMillian Island (Figure 2-7). The greatest change in volume (ΔV_{chan}) was observed between 1991 and 2003/2004 for the study area, where ~12x10^6 m^3 of degradation occurred at a rate of -1.6 Mt yr^{-1} (Figure 2-8). I assume a mineral density of 2650 kg/m^3 for silica sand and a sand porosity of 0.6 (van Rijn, 1993) which gives a bulk density of 1.59 tonnes/m^3 to convert sediment volumes (m^3) to a mass (Mt). There was also substantial change between 1951 and 1991, where 4.7x10^6 m^3 of degradation occurred, but at a lesser rate of -0.19 Mt yr^{-1}. Since 2003, ΔV_{chan} has been more modest in the reach, varying between +0.041 Mt yr^{-1} (aggradation) and -0.26 Mt yr^{-1} (degradation) (Figure 2-8). Despite a degradation dominated system, there some are notable areas with aggradation such as Bend 04 from 2003/2004 to 2010 and Bend 05 from 1952 to 1991, 1991 to 2003/2004, and 2003 to 2010 (Figure 2-8).

Figure 2-7. **Bed elevation difference map of the 2020/2021 and 1952 bed surface. The white areas highlight locations where negligible bed change occurred, while blue represents relative lowering and red represents relative deposition between the two surveys. Arrows indicate notable locations of bed aggradation.**

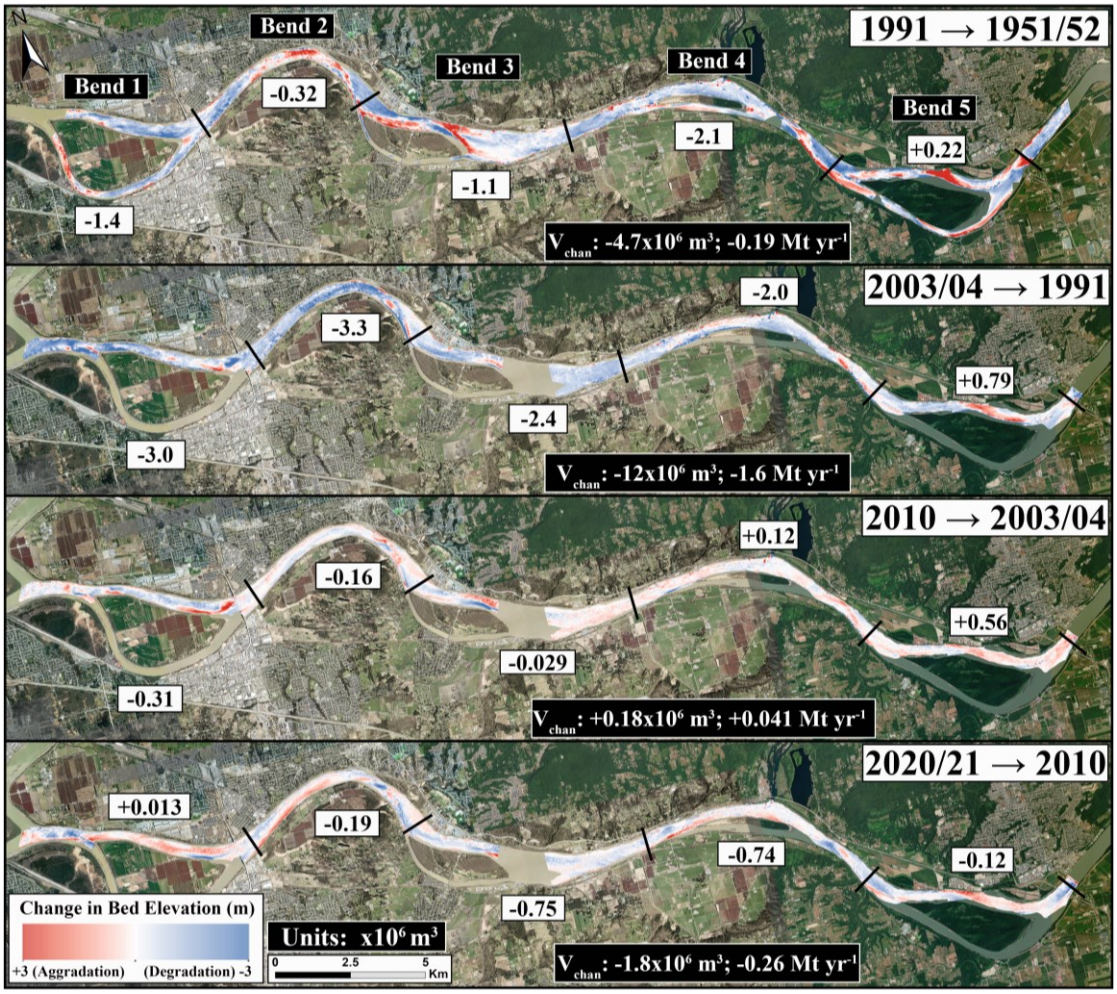

Figure 2-8. **Sequential difference maps of bed topography for the study area. For each bend segment a ΔV_{chan} value is recorded for the time interval associated with the panel. Additionally, the total ΔV_{chan} and a rate of degradation are recorded for the time period.**

The total cumulative ΔV_{chan} for the entire study reach was ~18x10^6 m^3 of degradation for the period of investigation (1951-2021) (Figure 2-9). Through Bends 01 to 04, ΔV_{chan} is similar, but there is aggradation in Bend 05. For the period of investigation (1951-2021), ΔV_{chan} was -0.41 Mt yr^{-1} (Figure 2-9).

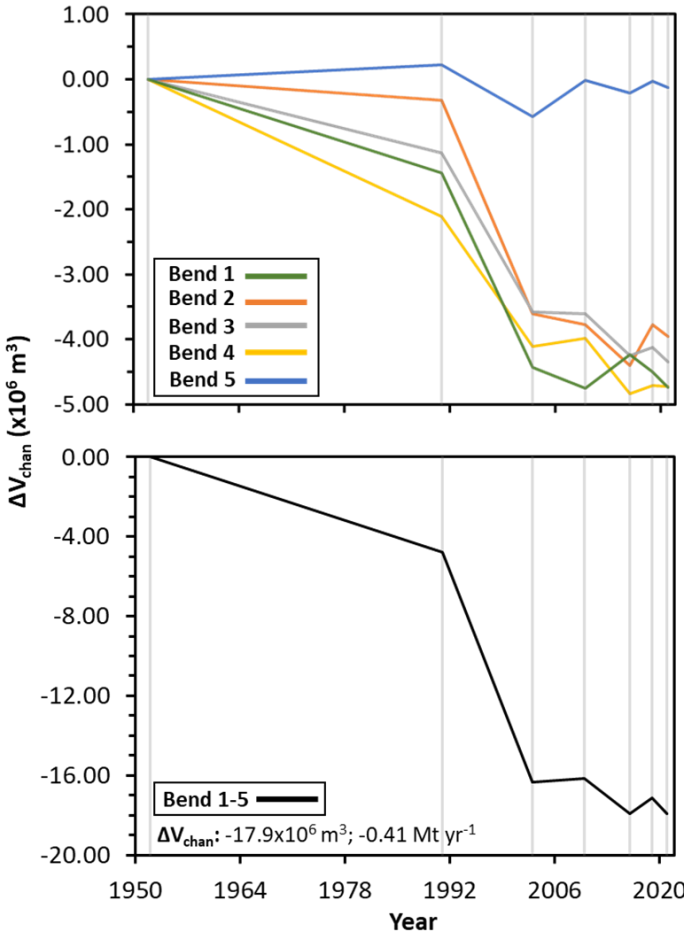

Figure 2-9. Cumulative ΔV_{chan} (x10^6 m^3) for the meander bend segments of the study reach. Bend locations are shown in Figure 8.

Long profiles of bed elevations for 1951/1952, 1991, 2003/2004, 2010, and 2021 further illustrate the change in bed level through the reach (Figure 2-10). For the overlapping areas where bed elevation data exists from ~RK 47 to 85 the change in average centerline bed elevation $\overline{\Delta\eta}$ from 1952 to 2021 was -0.93 m (Figure 2-10f). Bends 1 through 5 all recorded bed level lowering, but the lowering was more pronounced downstream (Figure 2-10a-e). From 1952 to 2021, $\overline{\Delta\eta}$ was almost 4 times greater in Bend 1 (-1.8 m) than in Bend 5 (-0.49 m), suggesting an upstream wave of incision.

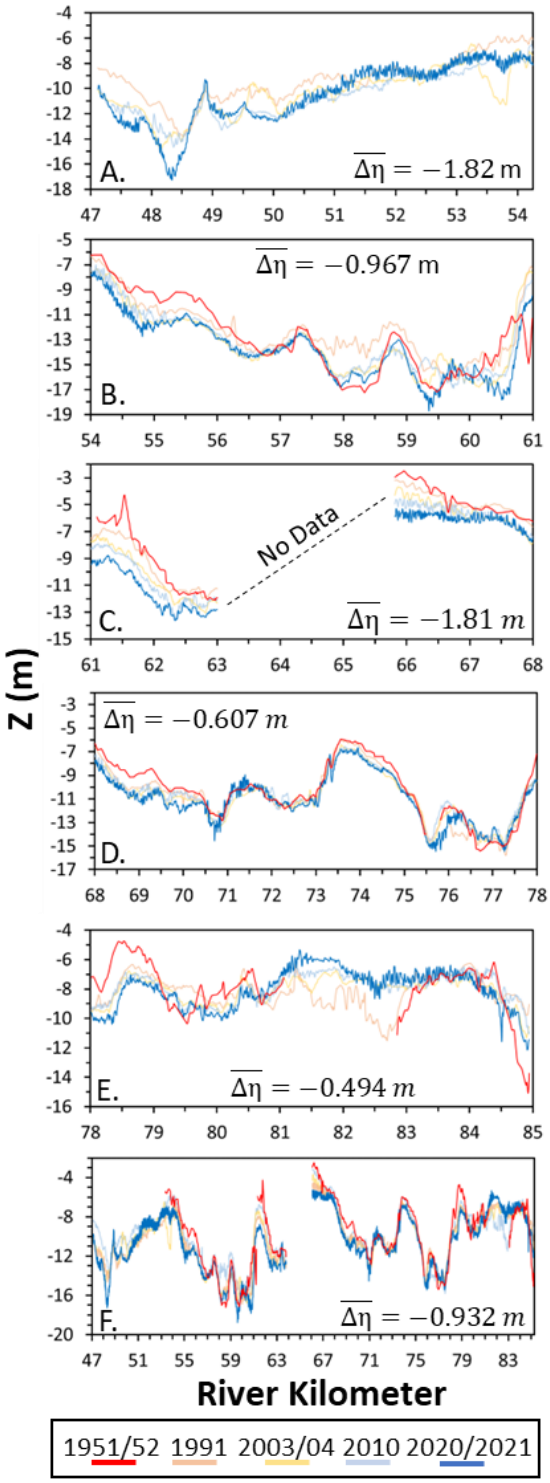

Figure 2-10. Centerline bed elevations (Z) for the 1951/1952, 1991, 2003/2004, 2010, 2020/2021 survey years for the bend segments (A-E) and the entire study area (F).

2.3.3. Dredging Volumes (V_{dredge})

There are two periods of relatively intense dredging in the Fraser Delta. The mean volume dredged from 1961 to 2013, the last year of reported dredging, was 2.9x10^6 m^3. From 1975 to 1991, an average of ~4.7x10^6 m^3 of sediment was removed from the system (7.5 Mt yr^{-1}) (Figure 2-11a). This period of intense dredging exceeds V_{in-h} (3.0 Mt yr^{-1}) and V_{in-c} (2.4 Mt yr^{-1}) (Figure 2-11a). The second period of intense dredging is from 2005 to 2013 when mean V_{dredge} = 3.0x10^6 m^3 of sediment being removed from the system annually (4.8 Mt yr^{-1}) (Figure 2-11a), which also exceeds V_{in-h} and V_{in-c} (Figure 2-11a). Since 2013, V_{dredge} is unknown, but the volume of dredged sand disposed at sea (V_{spoil}) increased from 0.484 in 2010 to a stable mean value of 1.76 from 2014 to 2020 (Figure 2-11b). The ratio γ (V_{dredge} to V_{spoil}) varied between 2.32 and 2.51 with a mean of 2.44 for 2010 to 2013, the only period of overlapping records. Applying this ratio using Equation (2-5), I estimate the contemporary (2010 to 2020) V_{dredge} to be 3.9x10^6 m^3 yr^{-1} which is equivalent to 6.2 Mt yr^{-1} (Figure 2-11b). Estimates of V_{dredge} from 2014 to 2020 suggests that the second period of increased dredging removals from 2005 to 2013 is still ongoing, with an estimated average of ~3.5x10^6 m^3 of sediment being dredged from the system annually from 2005 to 2020 at a rate of 5.5 Mt yr^{-1}. The current estimates of V_{dredge} exceeds V_{in-c} by ~130%.

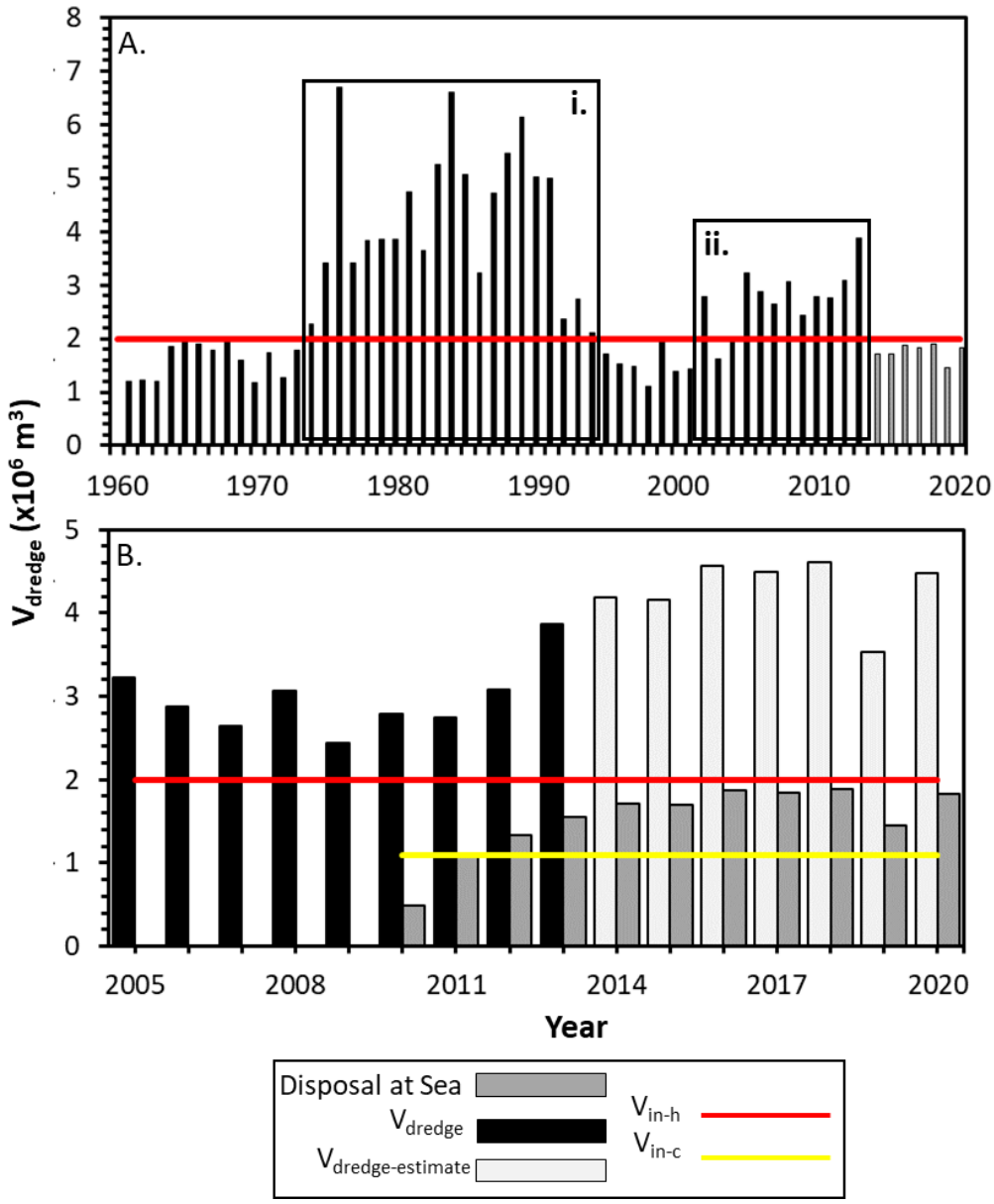

Figure 2-11. **(A) Sediment dredging time series based on published dredging records from 1961 to 2013 (black) and ECCC disposal at sea volumes from 2010 to 2020 (dark gray). The black boxes (i) and (ii) represent periods of intense dredging. (B) Sediment dredging time series from 2005 to 2020 showing the published dredging records from 2005 to 2013, ECCC disposal at sea records from 2010 to 2020, and dredging volume estimates from 2013 to 2020 (light gray). The red and yellow lines represents the historical (V_{in-h}) and contemporary (V_{in-c}) estimates of sediment supply to the lower Fraser River at Mission, British Columbia, respectively.**

2.3.4. Sediment Delivery to the Fraser Delta Channels ($V_{in-delta}$)

Sediment delivery to the Fraser Delta channels ($V_{in-delta}$) can be calculated as

$$V_{in-delta} = V_{in} - \Delta V_{chan} \qquad \text{Equation 2-10}$$

For the period from 1951 to 1966, I calculate V_{in} using the integration of the resulting values from Equation 2-7, and from 1966 to 2020, I use the V_{in} values which are summarized in Figure 2-6c. The ΔV_{chan} data from 1951 to 2021 is summarized in Figure 2-9. During the period of investigation from 1951 to 2020, $V_{in-delta}$ estimates ranged from 0.67 Mt yr^{-1} in 2010 when discharge peaked at 7,490 m^3 sec^{-1} to 9.1 Mt yr^{-1} in 1972 during an exceptionally high flood flow that had a peak discharge of 14,400 m^3 sec^{-1} (Figure 2-12a). Mean $V_{in-delta}$ was 3.8 Mt yr^{-1} prior to the intense period of dredging from 1975 to 1991. During intense dredging from 1975 to 1991 and from 2005 to 2013, $V_{in-delta}$ was 2.6 Mt yr^{-1} and 2.1 Mt yr^{-1} respectively. Since 2010, $V_{in-delta}$ = 2.2 Mt yr^{-1}.

2.3.5. Estimates of Sediment Output to the Delta Front (V_{out})

There are no direct observations of sediment output from the Fraser Delta at Sand Heads (RK 0) (V_{out}) but I can estimate V_{out} with a restated version of Equation 2-3

$$V_{out} = V_{in-delta} - \Delta V_{chan-delta} - V_{dredge} \qquad \text{Equation 2-11}$$

where $\Delta V_{chan-delta}$is the change in volume of the delta channels. I have no observations of annual $\Delta V_{chan-delta}$, but I can make a preliminary estimate of V_{out} by assuming that the Port of Vancouver dredging program maintains an approximately constant bed elevation in the navigational channel, which leads to a negligible $\Delta V_{chan-delta}$. Under this assumption, V_{out} ranges from 7.0 Mt in 1972 to -8.2 Mt in 1989 when V_{dredge} was ~10 Mt (Figure 2-12a). It is difficult to interpret a negative value of V_{out}. One interpretation is that there is no bed material sediment exiting the delta and that the negative V_{out} reflects a sediment deficit in the delta channels that is causing bed degradation (e.g., our assumption of $V_{chan-delta} = 0$ is incorrect). The net changes in the delta channels throughout the period of investigation can be better understood in terms of the cumulative change in $V_{in-delta}$ and V_{out} (Figure 2-12b). Starting in 1951, cumulative V_{dredge} is less than cumulative $V_{in-delta}$ until 1984 when cumulative V_{dredge}

exceeds cumulative $V_{in-delta}$ (Figure 2-12b). Since 1984, cumulative V_{dredge} has exceeded $V_{in-delta}$ (Figure 2-12b). However, from 1994 to 2010 the rate of $V_{in-delta}$ (3.0 Mt yr^{-1}) was similar to the rate of V_{dredge} (3.4 Mt yr^{-1}), but in 2005 the rate of V_{dredge} began increasing again outpacing $V_{in-delta}$ (Figure 2-12b). As of 2020, the cumulative volume of bed material sediment eroded from the delta channels is estimated to be ~90 Mt (Figure 2-12b).

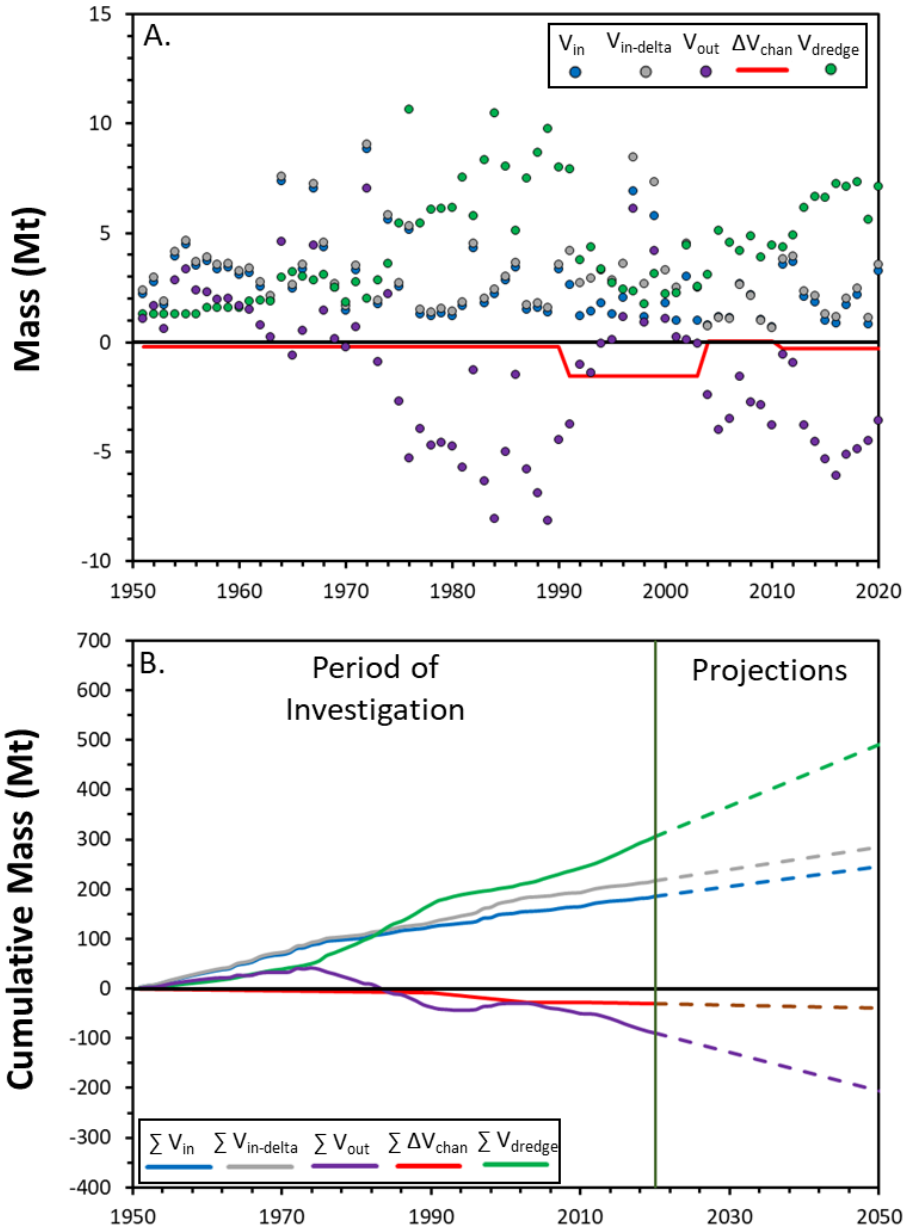

Figure 2-12. Annual (A) and cumulative (B) ΔV_{chan}, V_{dredge}, V_{in}, $V_{in-delta}$, and V_{out} estimates from 1951 to 2020 with projections to 2050, yielding a 100 year estimated sediment budget.

2.4. Discussion

2.4.1. Bed Degradation and Potential Causes

Bed degradation has been well documented in the Fraser River delta channels from New Westminster (RK 35) to Sand Heads (RK 0) (McLean et al., 2006; Nelson et al., 2017). However, a lack of recent bed topography data has prevented a detailed investigation of bed level change upstream of New Westminster. The results of this study show that bed degradation has occurred upstream of New Westminster from RK 47 (upstream of the Pitt River confluence) to Mission (RK 85) with a period of substantial bed degradation observed from 1991 to 2003/2004.

The bed degradation observed in the lower Fraser River may be the result of alterations to the natural profile of the riverbed initiated by sediment extractions to maintain draft depths associated with the navigational channel (McLean et al., 2006). Historically, the draft depth of the navigation channel in the delta channels has been increased through sediment extractions to account for large ocean-going vessels including the period of intense dredging from 1975 to 1991. From 2003 to 2006 the draft depth of the navigation channel was increased from 10.5 m to 11.7 m through the removal of 3.5×10^6 m^3 of sediment (Bros, 2007). Dredging of the river channel is generally concentrated downstream of New Westminster (RK 35). A dredge cut induced to the riverbed alters the natural slope of a riverbed which the channel must compensate for. Upstream of a dredge cut the gradient is steepened and a wave of degradation migrates upstream as the channel attempts to reach a new equilibrium. In the dredged zone, aggradation occurs and downstream the gradient of the riverbed is flattened.

Cumulative ΔV_{chan} for the study reach suggests that the riverbed may have made multiple adjustments to compensate for downstream changes in riverbed gradient. Bed degradation observed from 1991 to 2003/2004 in the study reach (RK 47 to 85) was preceded by a period of intense dredging from 1975 to 1991 in the reach downstream. The more recent bed degradation from 2010 to present was preceded by the increase in draft depth of the navigational channel from 10.5 m to 11.7 m, although the observed degradation was much less than the earlier period when the navigation channel was first established. Alternatively, the channel may be responding to a change in sediment supply to the reach where the capacity to transport sediment is greater than the

availability of sediment in the reach, but the changes in sediment supply to the reach appear to have occurred after the period of degradation.

2.4.2. Effects of a Sediment Supply Deficit to the Fraser Delta

The contemporary sediment fluxes recorded at Mission suggests that there has been a substantial reduction in sediment supply (V_{in}) to the lower Fraser River in recent years (Attard et al., 2014; Haught, 2017; Haught et al., 2020; Haught & Venditti, 2023). The reason for this shift in V_{in} is unknown, but it may be attributed to changes in precipitation and temperature throughout the Fraser River basin which affects the structure of the snowpack and timing of the freshet. These climatic changes may affect V_{in} because hillslopes in the Fraser River basin may be stabilizing, reducing the amount of sediment being introduced to the system and smaller annual snowpack's may reduce the frequency of large freshets. Additional considerations include changes to forest management practices which would result in better sediment retention and depletion of the sediment pulses associated with placer mining waste in the Fraser Canyon (e.g., Ferguson et al., 2015).

The delivery of bed material sediment to the delta channels ($V_{in-delta}$), which consists of the sediment load at Mission and the quantity of sediment removed from storage through bed degradation between Mission and New Westminster, has been reduced over the past 30 years. For the contemporary period (2010-2020) $V_{in-delta}$ = 2.0 Mt yr^{-1} (Figure 2-13). Yet, in the delta channels it is estimated that V_{dredge} = 6.2 Mt yr^{-1} for the contemporary period which results in a deficit of 3.9 Mt yr^{-1} of bed material in the delta channels (Figure 2-13). Based on the estimated values of $V_{in-delta}$ and V_{dredge} for the contemporary period, it is clear that $V_{dredge} > V_{in-delta}$.

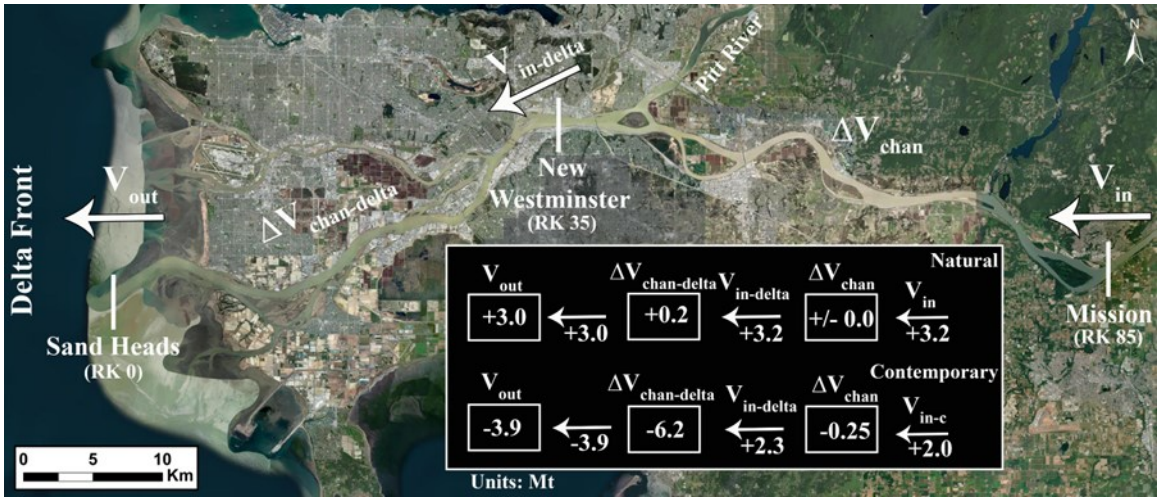

Figure 2-13. The estimated modern and contemporary bed material sediment budget for the lower Fraser River, British Columbia.

I can project the net change in the delta channel volume as a result of the dredging program assuming contemporary $V_{in-delta}$ and V_{dredge} remain unchanged. As of 2020, it was estimated that the cumulative volume of bed material lost from the delta channels was ~90 Mt (Figure 2-12b) which is equivalent to ~57x10^6 m^3 of bed material. Assuming the channel is ~35 km long stretching from New Westminster (RK 35) to Sand Heads (RK 0) and 0.5 km wide that is equivalent to ~3 m of bed material erosion. Nelson et al. (2017) observed ~3 m of degradation from RK 9 to RK 45 from 1974 to 2015, which is similar to our estimate. Therefore, if the current trends continue the delta channels will lose ~210 Mt of bed material (> 0.177 mm) by 2050 (Figure 2-12b), which is equivalent to ~8 m of erosion, to account for the sediment deficit in the channels. That degree of erosion is unlikely to occur without a major shift in delta channel dynamics.

The sediment budget for the contemporary period (2010-2020) can be used to estimate the net sediment deficit that produces negative V_{out} causing net delta channel degradation for various dredging scenarios. The contemporary estimates of sediment delivery (V_{in}), changes in upstream channel volume (ΔV_{chan}), and dredged volumes (V_{dredge}) produces a deficit in the delta of 3.9 Mt yr^{-1} (Figure 2-14). Figure 2-14a highlights how V_{out} might respond to various changes to the contemporary dredging regime. An end to the dredging program would eliminate the sediment deficit in the delta and create a sediment surplus of 2.2 Mt. Increasing dredging by 50% and returning to a V_{dredge} equivalent to the mid-1980's period of intense dredging would substantially increase the sediment deficit. Reducing dredging by 50% would substantially reduce the

deficit and a reduction by ~64% would potentially eliminate the sediment deficit and cease erosion of the delta channels. There appears to be no amount of dredging that would allow the natural sediment output of 3.2 Mt to be restored because a large volume of sediment from the drainage basin would be needed, in addition to ending the dredging program.

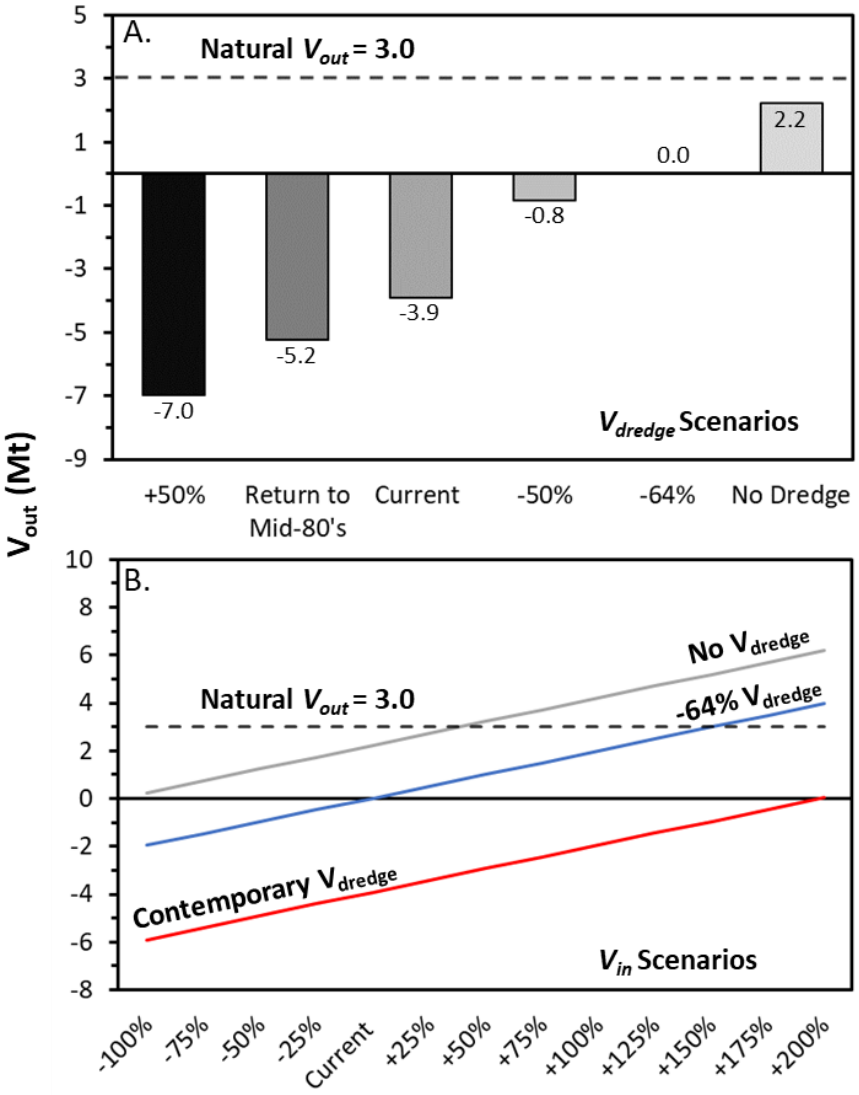

Figure 2-14. Different V_{dredge} (A) and V_{in} (B) scenarios and the impacts they have on V_{out}.

One way to balance the sediment budget and increase V_{out}, the natural sediment delivery to the ocean, would be for the sediment supply (V_{in}) to increase, which could occur due to changes in the basin and climate. Figure 2-14b highlights how the sediment

deficit would respond to changes in V_{in}. There is a linear increase in V_{out} with changes in V_{in}. Halving V_{in} would increase the deficit and enhance erosion in the delta channels. Doubling the sediment input would not be sufficient to balance the sediment budget. Based on the contemporary rates of V_{dredge}, V_{in} would have to increase by ~200% to eliminate the sediment deficit. If dredging ended, V_{in} would still have to increase by ~50% to restore V_{out} to natural levels. If dredging was reduced by 64%, the amount required to achieve a net zero sediment deficit, V_{in} would have to increase by ~150% to restore V_{out} to natural levels. Based on the reduction of V_{in} observed from the historic to contemporary sediment sampling periods, it is unlikely a substantial increase in V_{in} will occur in the future, highlighting the need to balance V_{dredge} against contemporary $V_{in-delta}$.

2.4.3. Future Work

The bed material sediment budget of the lower Fraser River and Delta has been estimated based on observations and estimations of sediment supply and storage changes through time. However, there are several limitations preventing an accurate assessment of the complete contemporary budget for the lower Fraser River and Delta. There are limited observations of sediment output to the Fraser Delta at Sand Heads (RK 0). Bedform migration and bedload transport rates through the delta channels have been estimated for high flows when most of the net sediment flux occurs (e.g., Kostaschuk et al., 1989; Villard & Church, 2003). There needs to be an effort to determine the sediment fluxes through the delta channels that includes measurements of the suspended bed material flux, the bedload transport, and the exchange between.

Sediment output from the delta channels is a major uncertainty in the present sediment budget. There have been some attempts to calculate sedimentation rates at the mouth of the main fluvial distributary and offshore of the tide flats (Mathews & Shepard, 1962; Evoy et al., 1993; Hart et al., 1998; Aryanci & Dashtgard, 2020). At the mouth, the sedimentation rate was calculated to be 13 cm yr^{-1}, while 4 km offshore the rate was < 3 cm yr^{-1}. In the Strait of Georgia, 300 m off the Fraser Delta, sedimentation rates associated with deep ocean renewals were calculated to be between 9 and 22.5 cm yr^{-1} (Aryanci & Dashtgard, 2020). How these sedimentation rates link to channel dynamics and sediment supply from upstream is not yet obvious and it is likely that

anthropogenic changes to the delta channels influence sedimentation rates in Strait of Georgia. For example, jetty construction at the mouth of the Main Arm and river training structures have prevented natural channel avulsion which is suspected to be causing asymmetry in accumulation rates, with higher sedimentation rates on the southern upper delta slope rather than the north (Hart et al., 1998).

All previous lower Fraser River sediment budget investigations, including this one, have rearranged the sediment budget equation to estimate sediment output to the delta front. An understanding of flow dynamics and sediment routing through the delta trifurcation and downstream to the delta front is necessary to constrain sediment output. Constraining sediment output will provide the framework necessary to assess the implications associated with a reduced bed material sediment load to the delta.

A permanent sediment monitoring station at Mission is necessary to further understand how much sediment is delivered to the system. Sediment flux monitoring using hydroacoustic instruments (ADCP) and methodologies have been applied to large rivers, including the Fraser River, making it a feasible and low-cost option (Haught, 2017; Haught et al., 2020; Haught & Venditti, 2023). Recent observations of sediment supply to the study reach are based on four years of data. The lower sediment loads observed during this period may be a result of sand accumulation and staging upstream of Mission (RK 85) and downstream of the GST (RK 100.5) that requires a major flood to mobilize and transport the sediment downstream (Venditti & Church, 2014). The contemporary flux data suggests a change in supply has occurred since the initial period of monitoring by the WSC that requires attention from a management perspective. Developing a consistent record of sediment supplied to the system will allow for a better understanding of sediment delivery and natural variations that will allow river managers to make more informed management decisions.

Targeted bed topography surveys through the rising, peak, and falling limbs of the hydrograph will provide the opportunity to better understand bedform migration and sediment staging through the different reaches of the lower Fraser (e.g., side channels, main channels, upstream of Mission). Surveys should not be limited to the navigational channel, bank to bank coverage is required to understand the complete picture of degradation, aggradation, and sediment routing through the channels. Understanding the dynamics of sediment staging and storage of sediment in the lower Fraser River will

allow for more directed sediment extractions in the delta channels. It is critical that targeted surveys continue regularly into the future and are systematically examined for trends of aggradation and degradation.

Lastly, the existing sediment budget and bed degradation studies focus on the Main Arm of the Fraser River and do not include the North and Middle Arm. Incorporating the Middle and North Arms into future studies is crucial for the overall management of the lower Fraser River and Delta. Additionally, compiling complete dredging records (e.g., volumes removed, location of disposal, date of removal, etc.) is required to accurately constrain the sediment budget of the Fraser River. From 2013 to present, besides the ECCC disposal at sea quantities, there are no complete records of the quantity of sediment being removed from the system.

2.5. Conclusions

Sediment flux at Mission (RK 85) and bed topography upstream of New Westminster from RK 47 to 85 were examined for the sand-bedded portion of the lower Fraser River. Surveys of the main channel from 1951/1952, 1991, 2003/2004, 2010, 2019, 2020/2021 provided an exceptional opportunity to examine change in bed elevation and sediment storage of the main channel which supplies the delta channels. Additionally, contemporary sediment flux measurements from 2010 to 2014 and updated dredging quantities and estimations allowed for an updated view of the lower Fraser River and Delta bed material sediment budget, while also highlighting areas that require further investigation. The results suggest that:

1. Observations of sediment flux at Mission from 2010 to 2014 show that the annual bed material load to the lower Fraser River has decreased through time with the historical flux data overpredicting the contemporary data by ~43% from 2010 to 2020.
2. The Main Arm of the lower Fraser River from RK 47 to 85 is generally degrading through time with a rate of -0.41 Mt yr^{-1} of degradation observed from 1951 to 2021. Degradation peaked from 1991 to 2003/2004 at a rate of -1.6 Mt yr^{-1} and has since been reduced.
3. The rate of contemporary dredging removals from 2010 to 2020 is estimated to substantially exceed the delivery of bed material sediment to the delta channels

resulting in a bed material sediment deficit that is likely causing erosion of the delta channels.

Further work is necessary to constrain the sediment dynamics in the delta channels and to measure sediment output to the Fraser Delta Front at Sand Heads, British Columbia.

References

Allen, J. R. L. (1965). A Review of the Origin and Characteristics of Recent Alluvial Sediments. *Sedimentology*, *5*, 89–191.

Allen, J. R. L. (1970). *Physical Processes of Sedimentation: An Introduction*. George Allen and Unwin LTD.

Allen, J. R. L. (1982). *Sedimentary Structures: Their Character and Physical Basis* (Vol. 2). Elsevier.

Allen, J. R. L. (1985). *Principles of Physical Sedimentation*. George Allen & Unwin.

Allison, M. A., Demas, C. R., Ebersole, B. A., Kleiss, B. A., Little, C. D., Meselhe, E. A., Powell, N. J., Pratt, T. C., & Vosburg, B. M. (2012). A water and sediment budget for the lower Mississippi–Atchafalaya River in flood years 2008–2010: Implications for sediment discharge to the oceans and coastal restoration in Louisiana. *Journal of Hydrology*, *432–433*, 84–97. https://doi.org/10.1016/j.jhydrol.2012.02.020

Almedia, R. P., Galeazzi, C. P., Freitas, B. T., Janikian, L., Ianniruberto, M., & Marconato, A. (2016). Large barchanoid dunes in the Amazon River and the rock record: Implications for interpreting large river systems. *Earth and Planetary Science Letters*, *454*, 92–102. https://doi.org/10.1016/j.epsl.2016.08.029

Aryanci, K., & Dashtgard, S. E. (2020). Deep-Water Renewal Events; Insights into Deep Water Sediment Transport Mechanisms. *Scientific Reports*, *10*. https://doi.org/10.1038/s41598-020-63123-3

Ashley, G. M. (1990). Classification of Large-Scale Subaqueous Bedforms: A New Look at an Old Problem. *Journal of Sedimentary Petrology*, *60*, 160–172.

Attard, M. E., Venditti, J. G., & Church, M. (2014). Suspended sediment transport in Fraser River at Mission, British Columbia: New observations and comparison to historical records. *Canadian Water Resources Journal*, *39*(3), 356–371. https://doi.org/10.1080/07011784.2014.942105

Bradley, R. W., & Venditti, J. G. (2017). Reevaluating dune scaling relations. *Earth-Science Reviews*, 356–376. http://dx.doi.org/10.1016/j.earscirev.2016.11.004

Bradley, R. W., & Venditti, J. G. (2021). Mechanisms of Dune Growth and Decay in Rivers. *Geophysical Research Letters*, *48*. https://doi.org/10.1029/2021GL094572

Bradley, R. W., Venditti, J. G., Kostaschuk, R. A., Church, M., Hendershot, M., & Allison, M. A. (2013). Flow and sediment suspension events over low-angle dunes: Fraser Estuary, Canada. *Journal of Geophysical Research: Earth Surface*, *118*, 1693–1709. https://doi.org/doi:10.1002/jgrf.20118

Bridge, J. S. (2003). *Rivers and Floodplains: Forms Processes and the Sedimentary Record*. Blackwell Science Ltd.

Bridge, J. S., & Jarvis, J. (1982). The Dynamics of a River Bend: A study in Flow and Sedimentary Processes. *Sedimentology*, *29*, 499–541.

British Columbia. (2017). *George Massey Tunnel Replacement Project—River Hydraulics and River Morphology Study*.

Bros, W. J. (2007). *Sustainable Dredging Program on the Lower Fraser River* [Master of Business Administration]. Simon Fraser University.

Church, M., McLean, D. G., & Wolcott, J. F. (1987). River-bed gravels: Sampling and Analysis. *Sediment Transport in Gravel-Bed Rivers: Proceedings of the 2nd International Gravel-Bed Rivers Workshop*.

Cisneros, J., Best, J., van Dijk, T., Paes de Almeida, R., Amsler, M., Boldt, J., Freitas, B., Galeazzi, C., Huizinga, R., Iannirubertо, M., Ma, H., Nittrouer, J. A., Oberg, K., Orfeo, O., Parsons, D. R., Szupiany, R., Wang, P., & Zhang, Y. (2020). Dunes in the world's big rivers are characterized by low-angle lee-side slopes and a complex shape. *Nature Geoscience*, 156–162.

Clague, J. J., Luternauer, J. L., & Hebda, R. J. (1983). Sedimentary environments and postglacial history of the Fraser Delta and lower Fraser Valley, British Columbia. *Canadian Journal of Earth Sciences*, *20*, 1314–1326. https://doi.org/10.1139/e83-116

de Lange, S. I., Naqshband, S., & Hoitink, A. J. F. (2021). Quantifying Hydraulic Roughness From Field Data: Can Dune Morphology Tell the Whole Story? *Water Resources Research*, *57*(12). https://doi.org/10.1029/2021WR030329

de Ruijsscher, T. V., Naqshband, S., & Hoitink, A. J. F. (2020). Effect of non-migrating bars on dune dynamics in a lowland river. *Earth Surface Processes and Landforms*, *45*, 1361–1375. https://doi.org/10.1002/esp.4807

Duan, N. (1983). Smearing Estimate: A Nonparametric Retransformation Method. *Journal of the American Statistical Association*, *78*(383), 605–610.

Evoy, R. W., Moslow, T. F., Patterson, R. T., & Luternauer, J. L. (1993). Patterns and variability in sediment accumulation rates, Fraser River delta foreslope, British Columbia, Canada. *Geo-Marine Letters*, *13*, 212–218.

Ferguson, R. I., Church, M. A., & Venditti, J. G. (2015). Reconstructing a sediment pulse: Modeling the effect of placer mining on Fraser River, Canada. *Journal of Geophysical Research: Earth Surface*, *120*(7), 1436–1454. https://doi.org/10.1002/2015JF003491

Galeazzi, C. P., Almedia, R. P., Mazoca, C. E., Best, J. L., Freitas, B. T., Ianniruberto, M., Cisneros, J., & Tamura, L. N. (2018). The significance of superimposed dunes in the Amazon River: Implications for how large rivers are identified in the rock record. *Sedimentology*, *65*, 2388–2403. https://doi.org/10.1111/sed.12471

Ham, D. G., & Church, M. A. (2012). Morphodynamics of an extended bar complex, Fraser River, British Columbia. *Earth Surface Processes and Landforms*, *37*, 1074–1089. https://doi.org/10.1002/esp.3231

Hart, B. S., Hamilton, T. S., & Barrie, J. V. (1998). Sedimentation rates and patterns on a deep-water delta (Fraser Delta, Canada); integration of high-resolution seismic stratigraphy, core lithofacies, and 137 Cs fallout stratigraphy. *Journal of Sedimentary Research*, *68*, 556–558.

Haught, D. W. (2017). *Acoustically Derived Suspended Sediment Concentrations and Flux in the Fraser River, Canada* [Doctor of Philosophy]. Simon Fraser University.

Haught, D. W., & Venditti, J. G. (2023). Acoustically-derived sediment-index methods in large rivers: Assessment of two acoustic inversion models. *Water Resources Research*.

Haught, D. W., Venditti, J. G., & Wright, S. A. (2017). Calculation of in situ acoustic sediment attenuation using off-the-shelf horizontal ADCPs in low concentration settings. *Water Resources Research*, *53*, 5017–5037. https://doi.org/10.1002/2016WR019695

Haught, D. W., Venditti, J. G., & Wright, S. A. (2020). Application of Multifrequency Acoustic Inversions Using Three Horizontally Profiling ADCPs. *Water Resources Research*, *56*, 23. https://doi.org/10.1029/2019WR025298

Hendershot, M. L., Venditti, J. G., Bradley, R. W., Kostaschuk, R. A., Church, M., & Allison, M. A. (2016). Response of low-angle dunes to variable flow. *Sedimentology*, 743–760. https://doi.org/doi: 10.1111/sed.12236

Hendershot, M. L., Venditti, J. G., Church, M., Bradley, R. W., Kostaschuk, R. A., & Alllison, M. A. (2018). Crestline bifurcation and dynamics in fluvial-dominated, tidally-influenced flow. *Sedimentology*, 2621–2636. https://doi.org/doi: 10.1111/sed.12480

Ilersich, S. A. (1992). *Bedforms and bedload transport: Evaluating rate equations in the Fraser River, British Columbia, Canada* [MSc thesis]. University of Guelph.

Jackson, R. G. (1975). Velocity—Bed-form—Texture patterns of meander bends in the lower Wabash River of Illinois and Indiana. *Geological Society of America Bulletin*, *86*, 1511–1522.

Kleinhans, M. G., Wilbers, A. W. E., Swaaf, A. D., & Van Den Berg, J. H. (2002). Sediment Supply-Limited Bedforms in Sand-Gravel Bed Rivers. *Journal of Sedimentary Research*, *72*(5), 629–640.

Kondolf, G. M., Schmitt, R. J., Carling, P., Darby, S., Arias, M., Bizzi, S., Castelletti, A., Cochrane, T. A., Gibson, S., Kummu, M., Oeurng, C., Rubin, Z., & Wild, T. (2018). Changing sediment budget of the Mekong: Cumulative threats and management strategies for a large river basin. *Science of The Total Environment*, *625*, 114–134. https://doi.org/10.1016/j.scitotenv.2017.11.361

Kostaschuk, R. A., & Church, M. A. (1993). Macroturbulence generated by dunes: Fraser River, Canada. *Sedimentary Geology*, *85*, 25–37. https://doi.org/10.1016/0037-0738(93)90073-E

Kostaschuk, R. A., Church, M. A., & Luternauer, J. L. (1989). Bedforms, bed material, and bedload transport in a salt-wedge estuary: Fraser River, British Columbia. *Canadian Journal of Earth Sciences*, *26*, 1440–1452. https://doi.org/10.1139/e89-122

Kostaschuk, R. A., & Venditti, J. G. (2019). Why do large, deep rivers have low-angle dune beds? *Geology*, *47*, 919–922. https://doi.org/10.1130/G46460.1

Kostaschuk, R. A., & Villard, P. (1996). Flow and sediment transport over large subaqueous dunes: Fraser River Canada. *Sedimentology*, 849–863. https://doi.org/10.1111/j.1365-3091.1996.tb01506.x

Levey, R. A. (1978). Bed-Form Distribution and Internal Stratification of coarse-grained point bars, Upper Congaree River, SC. *Can Soc Petrol Geol Mem 5*, 105–127.

Ma, H., Nittrouer, J. A., Fu, X., Parker, G., Zhang, Y., Wang, Y., Lamb, M. P., Cisneros, J., Best, J., Parsons, D. R., & Wu, B. (2022). Amplification of downstream flood stage due to damming of fine-grained rivers. *Nature Communications*.

Mathews, W. H., & Shepard, F. P. (1962). Sedimentation of Fraser River Delta, British Columbia. *Bulletin of the American Association of Petroleum Geologists*, *46*(8), 1416–1443. https://doi.org/10.1306/BC7438BB-16BE-11D7-8645000102C1865D

McLean, D. G., Church, M., & Tassone, B. (1999). Sediment transport along lower Fraser River 1. Measurements and hydraulic computations. *Water Resources Research*, *35*, 2533–2548.

McLean, D. G., Mannerstrom, M., & Lyle, T. (2006). Impacts of human interventions on the lower Fraser River. *Canadian Water Resources Association, British Columbia Division, Annual Conference*, 10.

McLean, D. G., & Tassone, B. (1991). A sediment budget of the Lower Fraser River. *5th Inter-Agency Sedimentation Conference*, 2–33 to 2–40.

Miall, A. D. (1996). *The Geology of Fluvial Deposits: Sedimentary Facies, Basin Analysis, and Petroleum Geology*.

Nelson, A. D., Klinghoffer, I., Gellis, M., & McLean, D. G. (2017). *Effect of Longterm Navigation Channel Lowering on Scour and Degradation Processes on Lower Fraser River*. HYD722-1-HYD722-10.

Nienhuis, J. H., Ashton, A. D., Edmonds, D. A., Hoitink, A. J. F., Kettner, A. J., Rowland, J. C., & Tornqvist, T. E. (2020). Global-scale human impact on delta morphology has led to net land area gain. *Nature*, *577*, 514–518.

Nittrouer, J. A., Allison, M. A., & Richard, C. (2008). Bedform transport rates for the lowermost Mississippi River. *Journal of Geophysical Research*, *113*. https://doi.org/doi:10.1029/2007JF000795

Northwest Hydraulic Consultants. (2002). *Review of lower Fraser River sediment budget: Final report*.

Parsons, D. R., Best, J. L., Orfeo, O., Hardy, R. J., Kostaschuk, R., & Lane, S. N. (2005). Morphology and flow fields of three-dimensional dunes, Rio Paraná, Argentina: Results from simultaneous multibeam echo sounding and acoustic Doppler current profiling. *Journal of Geophysical Research*, *110*. https://doi.org/10.1029/2004JF000231

Pretious, E. (1958). *Dredging on the Fraser River*. University of British Columbia.

Prokocki, E. W., Best, J. L., Perillo, M. M., Ashworth, P. J., Parsons, D. R., Sambrook Smith, G. H., Nicholas, A. P., & Simpson, C. J. (2022). The morphology of fluvial-tidal dunes: Lower Columbia River, OR/WA, USA. *Earth Surface Processes and Landforms*, *47*(8), 2079–2106. https://doi.org/10.1002/esp.5364

Public Works Canada. (1957). *Fraser River system, Province of British Columbia: History of improvements, 1871 to date* (p. 66). Public Works Canada.

Stein, R. A. (1965). Laboratory Studies of Total Load and Apparent Bed Load. *Journal of Geophysical Research*, *70*(8), 1831–1842.

Syvitski, J. P. M., Angel, J. R., Saito, Y., Overeem, I., Vorosmarty, C. J., Wang, H., & Olago, D. (2022). Earth's sediment cycle during the Anthropocene. *Nature Reviews Earth & Environment*, *3*, 179–196. https://doi.org/10.1038/s43017-021-00253-w

Syvitski, J. P. M., Anthony, E., Saito, Y., Zainescu, F., Day, J., Bhattacharya, J. P., & Giosan, L. (2022). Large deltas, small deltas: Toward a more rigorous understanding of coastal marine deltas. *Global and Planetary Change*, *218*. https://doi.org/10.1016/j.gloplacha.2022.103958

Syvitski, J. P. M., Vorosmarty, C. J., Kettner, A. J., & Green, P. (2005). Impact of Humans on the Flux of Terrestrial Sediment to the Global Coastal Ocean. *Science*, *308*.

van Rijn, L. C. (1993). *Principles of Sediment Transport in Rivers, Estuaries and Coastal Seas.* (Vol. 1006). Aqua Publications.

Venditti, J. G., & Bradley, R. W. (2022). Bedforms in Sand Bed Rivers. In *Treatise on Geomorphology* (2nd ed., Vol. 6, pp. 222–253). Elsevier.

Venditti, J. G., & Church, M. (2014). Morphology and controls on the position of a gravel sand transition: Fraser River, British Columbia. *Journal of Geophysical Research: Earth Surface*, *119*, 1959–1976. https://doi.org/10.1002/2014JF003147

Venditti, J. G., Church, M. A., & Bennett, S. J. (2005a). Morphodynamics of small-scale superimposed sand waves over migrating dune bed forms. *Water Resources Research*, *41*(10). https://doi.org/10.1029/2004WR003461

Venditti, J. G., Church, M. A., & Bennett, S. J. (2005b). On the Transition Between 2D and 3D Dunes. *Sedimentology*, 1343–1359. https://doi.org/doi: 10.1111/j.1365-3091.2005.00748.x

Venditti, J. G., Church, M., Attard, M. E., & Haught, D. W. (2016). Use of ADCPs for suspended sediment transport monitoring: An empirical approach. *Water Resources Research*, *52*, 2715–2736.

Venditti, J. G., Nittrouer, J. A., Allison, M. A., Humphries, R. P., & Church, M. A. (2019). Supply-limited bedform patterns and scaling downstream of a gravel–sand transition. *Sedimentology*, *66*, 2538–2556. https://doi.org/10.1111/sed.12604

Vermeulen, B., Hoitink, A. J. F., van Berkum, S. W., & Hldayat, H. (2014). Sharp bends associated with deep scours in a tropical river: The river Mahakam (East Kalimantan, Indonesia). *Journal of Geophysical Research: Earth Surface*, 1441–1454. https://doi.org/10.1002/2013JF002923

Villard, P., & Church, M. A. (2003). Dunes and associated sand transport in a tidally influenced sand-bed channel: Fraser River, British Columbia. *Canadian Journal of Earth Sciences*, *40*, 115–130. https://doi.org/10.1139/E02-102

Vishner, G. S. (1965). Fluvial Processes as Interpreted from Ancient and Recent Fluival Deposits. *S.E.M.P. Special Publications*, 116–132.

Wang, Z. Y., Li, Y., & He, Y. (2007). Sediment budget of the Yangtze River. *Water Resources Research*, *43*, 14. https://doi.org/10.1029/2006WR005012

Wasson, R. J. (2003). A sediment budget for the Ganga–Brahmaputra catchment. *Current Science*, *84*, 1041–1047.

Wu, S., Xu, Y. J., Wang, B., & Cheng, H. (2021). Riverbed dune morphology of the Lowermost Mississippi River—Implications of leeside slope, flow resistance and bedload transport in a large alluvial river. *Geomorphology*. https://doi.org/10.1016/j.geomorph.2021.107733

Yalin, M. S. (1964). Geometrical Properties of Sand Wave. *Journal of the Hydraulics Division*, *90*(5), 105–119. https://doi.org/10.1061/JYCEAJ.0001097

Zhou, L., Liu, J., Saito, Y., Diao, S., Gao, M., Qui, J., Xu, C., He, L., & Ye, S. (2020). Sediment budget of the Yellow River delta during 1959-2012, estimated from morphological changes and accumulation rates. *Marine Geology*, *430*, 14. https://doi.org/10.1016/j.margeo.2020.106363

Zomer, J. Y., Naqshband, S., Vermuelen, B., & Hoitink, A. J. F. (2021). Rapidly Migrating Secondary Bedforms Can Persist on the Lee of Slowly Migrating Primary River Dunes. *Journal of Geophysical Research: Earth Surface*, *126*(3). https://doi.org/10.1029/2020JF005918